Available online at www.sciencedirect.com
SCIENCE DIRECT®
Journal of Organometallic Chemistry 664 (2002) 5–26
Journal of Organometallic Chemistry
www.elsevier.com/locate/jorganchem

Indenyl-amido titanium and zirconium dimethyl complexes: improved synthesis and use in propylene polymerization

Luigi Resconi [a,*], Isabella Camurati [a], Cristiano Grandini [a,1], Marilisa Rinaldi [a,2], Nicoletta Mascellani [b], Orazio Traverso [b]

[a] *Basell Polyolefins, Centro Ricerche G. Natta, CER 158 P.le G. Donegani 12, I-44100 Ferrara, Italy*
[b] *CNR-Centro di Studio su Fotoreattività e Catalisi, Dipartimento di Chimica dell'Università di Ferrara, Via L. Borsari 46, I-44100 Ferrara, Italy*

Received 2 April 2002; accepted 12 August 2002

Abstract

The synthesis of a series of indenyl amido titanium dimethyl complexes, by means of the direct synthesis from the ligand, a 2-fold excess of MeLi, and $TiCl_4$ is reported. The ^1H NMR spectra of the complexes show a quartet structure for the metal-bound methyl groups, due to through-metal proton–proton coupling. Coupling of Ti-methyl protons with protons on the Cp ring is also revealed by COSY 2D-NMR. The performance of the Ti complexes in propylene polymerization, including $[Me_2Si(Me_4C_5)(t\text{-BuN})]TiMe_2$ (**1-TiMe$_2$**), $[Me_2Si(Ind)(t\text{-BuN})]TiMe_2$ (**2-TiMe$_2$**) and six other methyl titanium complexes bearing substituted indenyl ligands, has been investigated with different cocatalysts and at different polymerization temperatures and propylene concentrations. All complexes produce amorphous polypropylene (*am*-PP). The catalytic activity and molecular weight strongly depend on the substitution of the Cp ring: **2-TiMe$_2$** gives polymers of lower molecular weight, while the presence of a methyl group in position 2 (as in **3-TiMe$_2$**) determines up to 4-fold increase in molecular weight. The type of cocatalyst influences mainly the catalytic activity, the borates being better activators than MAO, but also molecular weight, with again the borates giving higher molecular weights than MAO. **5-TiMe$_2$**–$Ph_3CB(C_6F_5)_4$ shows an overall activation energy of polymerization of 7.35 kcal mol^{-1}. The rate of chain release is first order in monomer. The following activation energies for overall chain release have been calculated: $\Delta\Delta E^{\ddagger}$ **2-TiMe$_2$** = 3.4 kcal mol^{-1}, $\Delta\Delta E^{\ddagger}$ **5-TiMe$_2$** = 3.8 kcal mol^{-1}, $\Delta\Delta E^{\ddagger}$ **3-TiMe$_2$** = 6.3 kcal mol^{-1}. Even if all the polymers produced are amorphous, **2-TiMe$_2$** and **5-TiMe$_2$** show a microstructure unbalanced towards isotacticity, while **3-TiMe$_2$**, **6-TiMe$_2$** and **8-TiMe$_2$** are syndiotactic-enriched. Chiral induction comes mainly from a weak enantiomorphic site control.

Keywords: Indenyl amido titanium dimethyl complexes; Amorphous polypropylene

1. Introduction

As part of our continuing interest in amorphous polypropylenes (*am*-PP) [1–6], we are investigating known and new Group 4 metal complexes with the aim of finding catalysts able to produce *am*-PP with varying degrees of microstructures and molecular weights, properties that determine the processability and miscibility of this polyolefin with, for example, isotactic [2,4,5] or syndiotactic polypropylenes [3,4,6].

One of the reference catalysts for the production of high molecular weight *am*-PP is the so-called 'constrained geometry' titanium complex $[Me_2Si(Me_4C_5)(t\text{-BuN})]TiCl_2$ (**1-TiCl$_2$**) that is used with either AlR_3–$B(C_6F_5)_3$ or methylalumoxane (MAO) as cocatalysts [7–13].

Both **1-TiCl$_2$** and $[Me_2Si(Me_4C_5)(t\text{-BuN})]ZrCl_2$ (**1-ZrCl$_2$**) have been extensively investigated, and the results show that Ti is clearly superior to Zr within this family of complexes [7–13]. Ligand variations, on the Cp as well as on the type of bridge and the amide substituent, have been pursued. Previous studies by Canich [14] and Waymouth [15] have shown that the

* Corresponding author
E-mail address: luigi.resconi@basell.com (L. Resconi).
[1] Present address: FIS Fabbrica Italiana Sintetici, v.le Milano 26, I-36075 Montecchio Maggiore, Vicenza, Italy.
[2] Present address: Glaxo Wellcome Medicines Research Center, via Fleming 4, I-37135 Verona, Italy.

0022-328X/02/$ - see front matter
PII: S0022-328X(02)01853-3

Cp substitution pattern has limited influence on the stereoregularity of polypropylene, while both regioregularity and molecular weights are affected to a greater extent. The nature of the bridge affects the catalytic activity in propylene polymerization and, to a minor degree, the polymer microstructure [16]. The steric bulk of the amido substituent generally affects the polymer molecular weight, in a manner, which depends on Cp substitution and monomer type [14,15,17].

The influence of the cocatalyst was also addressed in different studies, although in this case the differences are less clear-cut [18,19].

In order to screen the influence of the π ligands on PP microstructure and molecular weight, we needed a simple and reliable method for the synthesis of different complexes. We have recently reported the successful preparation of a series of dimethylmetallocenes, by means of a one-pot synthesis from the ligand, a 2-fold excess of MeLi, and $MtCl_4$ (Mt = Ti, Zr, Hf) [20–23]. The same protocol was successfully applied to the synthesis of the dimethylsilylcyclopentadienyl amido complexes of both Zr and Ti, such as [$Me_2Si(Me_4C_5)(t\text{-BuN})$]$TiMe_2$ (**1-TiMe$_2$**) and [$Me_2Si(Me_4C_5)(t\text{-BuN})$]$ZrMe_2$ (**1-ZrMe$_2$**) [21].

We describe here the application of this simplified protocol to the synthesis of a series of indenyl amido titanium complexes, which differ in the substituents on indene. We also describe the results of propylene polymerization, in both liquid monomer and solution, with different cocatalysts and under different polymerization conditions.

2. Results and discussion

2.1. Synthesis of the complexes

1-TiCl$_2$ has been previously obtained in overall 32% yield from the dilithium salt of the ligand [24], or in 52% yield from the ligand dimagnesium salt [8,15]. Alternatively, **1-TiCl$_2$** can be prepared in quantitative yield by reaction of the ligand dimagnesium salt (obtained in 79% yield) with Ti(O-*i*-Pr)$_4$, followed by reaction with $SiCl_4$ in an overall yield of about 77% from the ligand [8]. **1-TiMe$_2$** was also obtained from [$Me_2Si(Me_4C_5)(t\text{-BuN})$]Ti(O-*i*-Pr)$_2$, by reaction of the latter with excess $AlMe_3$ (100% yield) [8]. The synthesis of **1-ZrCl$_2$** proceeds in better yield (85% from $ZrCl_4(THF)_2$ and the dilithium salt of the ligand) [10] while the dimethyl derivative **1-ZrMe$_2$** has not been reported so far.

With our method, at room temperature, we obtained **1-ZrMe$_2$** in high yield (89%, entry 2 in Table 1). The analogous, catalytically more important **1-TiMe$_2$** was obtained in 70% yield, which is notably higher than the yields obtained in the conventional three-step procedure [24]. The latter method requires the use of $TiCl_3(THF)_3$ followed by oxidation, because $TiCl_4$ leads to metal reduction [12]. In our case, $TiCl_4$ could be used without problems, since extensive reduction was not observed. This result shows that also Ti complexes of commercial relevance can be produced conveniently with our procedure.

We then turned our attention to the related (Ind)Si-Me_2(*t*-BuNH) ligand, which has been investigated by Stevens et al. [7], Herrmann [9], Okuda [11] and Waymouth [15] in the synthesis of asymmetric 'constrained geometry' catalysts. Following the procedure described by Stevens et al. [7], we have first obtained (1-indenyl)dimethylchlorosilane in 89% yield, free from its vinylic isomer but contaminated by 4% bisindenyldimethylsilane; then the final indenyldimethyl(*t*-BuNH)silane ligand was obtained in 83% yield, in a 75:25 ratio of its allylic and vinylic isomers (Scheme 1).

Okuda reported that conversion of the ligand to the [$Me_2Si(Ind)(t\text{-BuN})$]$TiCl_2$ complex occurs in 94% yield following the reaction sequence of Scheme 1, while the following methylation with MeMgCl at −78 °C gave [$Me_2Si(Ind)(t\text{-BuN})$]$TiMe_2$ as a yellow oil in 49% yield [11]. Stevens et al. [7] and Waymouth et al. [15] on the other side reported yields of 20–25% using salt metathesis between the $TiCl_4(THF)_2$ adduct and the dilithio salt of the ligand. [$Me_2Si(Ind)(t\text{-BuN})$]$ZrCl_2$ has been analogously prepared by Stevens et al. [7], by reaction of $ZrCl_4(THF)_2$ with the dilithio salt of indenyldimethyl(*t*-butylamido)silane in 36% yield, while [$Me_2Si(Ind)(t\text{-BuN})$]$ZrMe_2$ has not been reported so far. The related [$Me_2Si(Ind)(t\text{-BuN})$]$Ti(NMe_2)_2$ and [$Me_2Si(Ind)(t\text{-BuN})$]$Zr(NEt_2)_2$ have been prepared by Herrmann in quantitative yield from the corresponding tetrakis(dialkylamido)metals [9].

In our hands with the one-pot method, the novel [$Me_2Si(Ind)(t\text{-BuN})$]$ZrMe_2$ (**2-ZrMe$_2$**) was obtained as a brown solid in 90% yield after extraction, while [$Me_2Si(Ind)(t\text{-BuN})$]$TiMe_2$ (**2-TiMe$_2$**) could be isolated in 70% yield as a dark yellow powder. Analogously, six other Ti dimethyl complexes have been prepared in yields from 61 to 87%. The complexes prepared and reaction yields are listed in Table 1. All samples were purified by a single filtration, yielding dark colored pentane or toluene solutions from which the complexes were isolated by removing the solvents under reduced pressure. Due to the very high solubility of these dimethyl complexes, **1-TiMe$_2$**-**8-TiMe$_2$** have been tested as precatalysts in the polymerization of propylene without further purification.

The indenyl complexes studied in this work are shown in Chart 1.

2.2. NMR characterization

^1H and ^{13}C chemical shifts of protons and carbons on the indenyl fragment as well as on Si and Mt are listed in

Table 1
All reactions were carried out at room temperature

Label	Complex	Purity (%wt., ^{1}H-NMR)	Yield (%) [a]
1-TiMe$_2$	[Me$_2$Si(Me$_4$C$_5$)(*t*-BuN)]TiMe$_2$	> 95	70
1-ZrMe$_2$	[Me$_2$Si(Me$_4$C$_5$)(*t*-BuN)]ZrMe$_2$	> 98	89
2-TiMe$_2$	[Me$_2$Si(Ind)(*t*-BuN)]TiMe$_2$	> 97	70
2-ZrMe$_2$	[Me$_2$Si(Ind)(*t*-BuN)]ZrMe$_2$	> 98	90
3-TiMe$_2$	[Me$_2$Si(2-MeInd)(*t*-BuN)]TiMe$_2$	> 98	70
4-TiMe$_2$	[Me$_2$Si(3-*t*-BuInd)(*t*-BuN)]TiMe$_2$	85	66
5-TiMe$_2$	[Me$_2$Si(4,7-Me$_2$Ind)(*t*-BuN)]TiMe$_2$	96	61
6-TiMe$_2$	[Me$_2$Si(3-PhInd)(*t*-BuN)]TiMe$_2$	90	79
7-TiMe$_2$	[Me$_2$Si(2-Me-4-PhInd)(*t*-BuN)]TiMe$_2$	85	86
8-TiMe$_2$	[Me$_2$Si(2-Me-Benz[e]Ind)(*t*-BuN)]TiMe$_2$	> 96	87

[a] % Weight isolated yield, not corrected by purity.

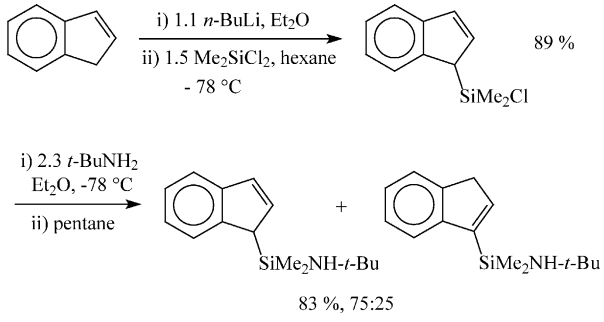

Scheme 1.

Table 2a and b, respectively. The assignments follow the numbering scheme shown in Chart 2, for **2-MtMe$_2$** (Mt = Ti, Zr)-**7-TiMe$_2$**, and in Chart 3 for **8-TiMe$_2$**.

The spectra of **2-MtMe$_2$** (Mt = Ti, Zr)-**8-TiMe$_2$** show some common features. The assignments of the ^{1}H-NMR spectra are based on the bidimensional COSYgs [29] and NOESY [30] spectra. The proton spectra of **2-MtMe$_2$** are compared in Fig. 1. In the proton spectra, the two methyls on ^{29}Si are identified from the peak multiplicity as they present at the base a doublet due to their coupling with ^{29}Si ($I = 1/2$, natural abundance = 4.7%).

A peculiarity of the ^{1}H-NMR spectrum of the titanium complexes is the quartet structure (a broad singlet if resolution is not good enough) showed by the metal-bound methyl groups. The COSY experiments show a proton–proton coupling between the two methyl groups on the metal, accounting for the multiplicity of the signal. A coupling with titanium can be reasonably excluded since the observed quartet is clearly due to the coupling with a nucleus of nearly 100% abundance, while Ti has a low isotopic abundance (^{47}Ti = 7.4%, ^{49}Ti = 5.4%).

Moreover, coupling of Ti-methyl protons with protons on the Cp ring is also present. The presence of through-metal homo- and heteronuclear long-range couplings was already observed in the case of *meso*-[C$_2$H$_4$(4,7-Me$_2$-1-Ind)$_2$]ZrMe$_2$ [20].

A coupling between protons H**3** and H**7** in **2-MtMe$_2$** (Mt = Ti, Zr), **3-TiMe$_2$**, **7-TiMe$_2$**, **8-TiMe$_2$** is usually observed owing to a long range coupling (J^5) typical of indenyl systems [25].

The ^{13}C-NMR spectra are assigned from DEPT-135, ^{1}H–^{13}C HSQC and ^{1}H–^{13}C HMBC 2D experiments. Protonated carbons are assigned from their cross peaks with directly bonded protons in the ^{1}H–^{13}C HSQC spectrum [26,27]; for quaternary carbons ^{1}H–^{13}C HMBC 2D spectra [28] are used.

In the ^{1}H–^{13}C HMBC spectra the quaternary carbon of the *t*-Bu is identified from the cross-peaks with its methyl protons, the carbon C**1** is identified from its cross-peaks with Si-methyl protons and with the proton or the methyl protons in position 2.

For more detailed NMR data see the Section 5.

2.3. Propylene polymerization

In order to evaluate to what extent different substituents on the indenyl ring can influence catalyst performance, we tested complexes **2-TiMe$_2$**-**8-TiMe$_2$** in propylene polymerization under a variety of conditions. Selected polymerization results from **1-TiCl$_2$** and **1-TiMe$_2$** –MAO catalysts are also reported for comparison.

Polymerizations in both liquid monomer and in solution were performed to compare catalytic activity, polymer microstructure and molecular weight. Different cocatalysts, namely methylalumoxane (MAO), triphenylcarbenium tetrakis(pentafluorophenyl)borate ([Ph$_3$C][B(C$_6$F$_5$)$_4$]), *N,N*-dimethylanilinium tetrakis(pentafluorophenyl)borate ([PhNHMe$_2$][B(C$_6$F$_5$)$_4$]) and tris(pentafluorophenyl)borane (B(C$_6$F$_5$)$_3$), were tested to study the effect of different counterions on catalyst behavior. For some of the catalysts we carried out a deeper investigation by changing polymerization temperature and monomer concentration.

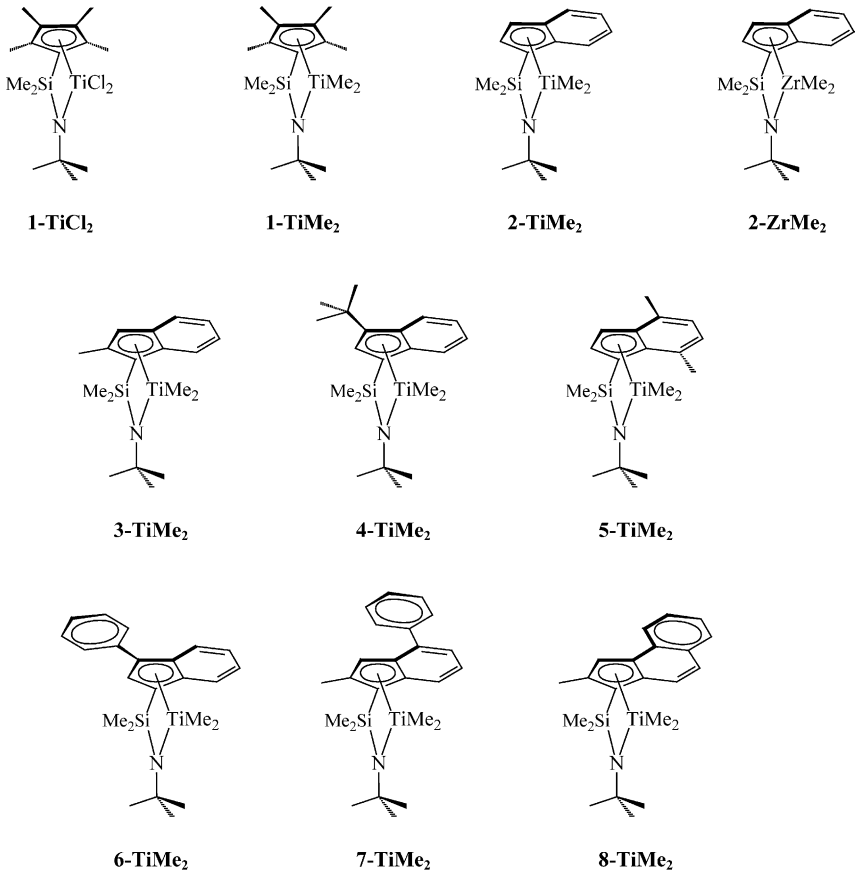

Chart 1. The complexes of the present study.

2.3.1. Propylene polymerization in liquid monomer with MAO cocatalyst

The polymerization results from MAO-activated Ti complexes **1-TiX$_2$** (X = Cl, Me), **2-TiMe$_2$**, **3-TiMe$_2$**, **7-TiMe$_2$** and **8-TiMe$_2$** are compared in Table 3. **4-TiMe$_2$** and **6-TiMe$_2$** showed no or very low activity (test not reported in Table 3) and were not further investigated. As expected, **1-TiCl$_2$** and **1-TiMe$_2$** behave identically in terms of catalyst activity and molecular weight and tacticity of the polymer. All other catalysts produce *am*-PP with molecular weights that are strongly influenced by the substitution of the Cp ring and polymerization temperature, and only marginally by the MAO/Ti ratio. Catalysts activities are on the low side, when compared with MAO-activated metallocenes [1]. As observed by Waymouth [15], the unsubstituted indenyl ligand in **2-TiMe$_2$** induces relatively low molecular weights, even under liquid monomer conditions (see runs 9 and 10 in Table 3). As shown by Spaleck and coworkers for C_2-symmetric *ansa*-zirconocenes [31], substituting 2-MeInd for Ind as in **3-TiMe$_2$**, **7-TiMe$_2$** and **8-TiMe$_2$** generates up to 4-fold increase in molecular weight (compare runs 9–10 with 11–13 in Table 3). For PP from **8-TiMe$_2$** the molecular weight is lower than expected, although higher than that made with **2-TiMe$_2$**. In turn, **8-TiMe$_2$** shows the highest catalytic activity. The tetramethylcyclopentadienyl ligand affords the highest molecular weights.

The most representative propylene polymers have been analyzed by ^{13}C-NMR. The triad content, racemic dyad excess (% rde [32,33]) and triad tests (*E* and *B* [32,33]) for the determination of the stereocontrol mechanism are reported in Table 3. The methyl pentad region of the spectrum of sample 3 is shown in Fig. 2. The methyl region of spectra of *am*-PP produced by two metallocene-based catalysts, *meso*-$C_2H_4(H_4Ind)_2ZrCl_2$–MAO [1], and *rac*-$CH_2(3\text{-}i\text{Pr-Ind})_2ZrCl_2$–MAO [2], are also shown for comparison in the Fig. 2.

It is apparent that *am*-PP produced with **1-TiCl$_2$** (and **1-TiMe$_2$**), although amorphous, have a syndiotactic-enriched microstructure, in accordance with the finding of Waymouth [15]. Longer syndiotactic sequences (*rrrrrr*) can be observed, although the triad distribution does not enable us to tell what mechanism is operating with this catalysts. On the other side, the very low level of *mmmm* sequences is not consistent with the existence of tight ion pairs during monomer insertion. **1-TiCl$_2$** shows a negligible effect of polymerization temperature on syndiotacticity, while a strong effect on molecular weight can be noted.

Both **2-TMe$_2$**, sporting the unsubstituted indenyl ligand, and **7-TMe$_2$** produce nearly atactic PP: the

Table 2
Chemical shift (ppm)

Complex	C**2**-C$\underline{H}_3$	H**2**	H**3**	H**4**	H**5**	H**6**	H**7**	H**8** Si–C$\underline{H}_3$ in	H**9** Si–C$\underline{H}_3$ out	H**10** Mt–C$\underline{H}_3$ in	H**11** Mt–C$\underline{H}_3$ out	
(a) ^{1}H												
2-TiMe$_2$	–	6.05	7.01	7.48	7.07	6.88	7.46	0.53	0.36	−0.15	0.82	
2-ZrMe$_2$	–	6.31	6.68	7.39	7.03	6.92	7.58	0.40,0.60		−0.74	0.24	
3-TiMe$_2$	1.99	–	6.76	7.44	7.07	6.89	7.51	0.56	0.46	−0.11	0.85	
4-TiMe$_2$	–	6.15	–	7.81	7.11	6.84	7.53	0.63	0.38	−0.12	0.99	
5-TiMe$_2$	–	6.19	7.09	–	6.83	6.71	–	0.57	0.39	−0.19	0.78	
6-TiMe$_2$	–	6.39	–	7.96	7.08–7.18	6.92	7.53	0.61	0.42	0.0065	0.68	
7-TiMe$_2$	1.95	–	7.20	–	7.11–7.32	6.97	7.52	0.60	0.47	0.005	0.85	
8-TiMe$_2$	2.06	–	7.30	–	–	7.21	7.44	0.60	0.49	−0.33	0.83	
Complex	**C1**	**C2**-C$\underline{C}H_3$	**C2**	**C3**	**C4**	**C5**	**C6**	**C7**	**C8** Si–C$\underline{C}H_3$ in	**C9** Si–C$\underline{C}H_3$ out	**C10** Mt–C$\underline{C}H_3$ in	**C11** Mt–C$\underline{C}H_3$ out
(b) ^{13}C												
2-TiMe$_2$	91.86	–	126.84	114.12	125.94	126.07	125.48	127.63	3.96	1.84	57.18	53.85
3-TiMe$_2$	89.61	17.98	140.97	115.64	124.90	125.17	124.72	127.81	5.55	5.30	56.57	50.82
4-TiMe$_2$	90.05	–	120.98	141.03	126.08	125.25	124.54	127.80	4.60	1.81	57.89	54.46
5-TiMe$_2$	92.58	–	128.35	112.32	132.49	125.71	126.71	135.51	5.71	3.48	56.52	52.03
6-TiMe$_2$	92.95	–	124.54	129.62	124.62	126.65	125.44	128.00	4.09	1.82	56.33	59.10
7-TiMe$_2$	89.99	18.51	141.90	115.73	139.17	125.35	125.75	126.26	6.00	5.58	57.62	51.88
8-TiMe$_2$	92.62	18.42	139.85	114.86	131.21	129.22 or 132.35	126.84	124.83	6.01	5.71	56.71	50.80

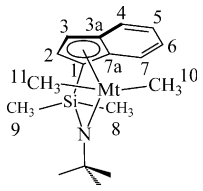

Chart 2. Mt = Ti, Zr.

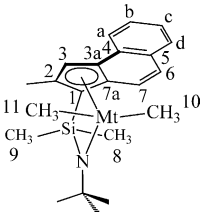

Chart 3. **8-TiMe$_2$**. The peak numbering does not follow the correct IUPAC numbering, to allow for an easier comparison with the structures of the other complexes.

triads *mm* and *rr* are very similar to each other, and the % rde, although higher than zero, are the lowest, to indicate a marginal tendency toward syndiotacticity. In all other cases, the tendency toward syndiotacticity becomes more marked, following the order **1-TiMe$_2$** ~ **1-TiCl$_2$** > **8-TiMe$_2$** > **3-TiMe$_2$** > **2-TiMe$_2$** > **7-TiMe$_2$**. With the exception of **3-TiMe$_2$** and **8-TiMe$_2$**, all catalysts produce relatively high levels of 2,1-insertions, higher than observed in the corresponding *ansa*-zirconocenes [1].

2.3.2. Propylene polymerization in solution: influence of cocatalyst

MAO-activated **3-TiMe$_2$**, **5-TiMe$_2$** and **6-TiMe$_2$** were also tested at 50 °C in toluene under 3 bar-g of propylene pressure. For **3-TiMe$_2$**, as expected at lower propylene concentration catalyst activities and molecular weights decrease, while the microstructure remains unchanged.

Given the low activity observed at low pressure for the MAO-activated complexes, the eight Ti complexes were also tested in toluene with [Ph$_3$C][B(C$_6$F$_5$)$_4$] as cocatalyst and Al(*i*Bu)$_3$ as scavenger. The results are reported in Table 4. Again, **4-TiMe$_2$** proved almost inactive, followed by **6-TiMe$_2$**. In addition, the latter also produces the lowest molecular weights of all catalysts investigated. Hence, we focused our attention on **2-TiMe$_2$**, **3-TiMe$_2$** and **5-TiMe$_2$**. The tests performed with these three complexes activated by [PhNHMe$_2$]-[B(C$_6$F$_5$)$_4$] are also reported in Table 4. Polymerization experiments were also carried out with B(C$_6$F$_5$)$_3$ as the activator, but under our chosen conditions it resulted completely inactive (tests not reported in Table 4). Some authors have already reported the noticeable activity increase from B(C$_6$F$_5$)$_3$ to [Ph$_3$C][B(C$_6$F$_5$)$_4$] [18,34–37], which they attributed to the higher coordination ability of [MeB(C$_6$F$_5$)$_3$]$^-$ compared with [B(C$_6$F$_5$)$_4$]$^-$. In combination with 'constrained geometry' catalysts this interaction could be so strong to prevent the displacement of the anion by the olefin, giving essentially inactive species.

While **1-TiCl$_2$** is the most active catalyst, among the indenyl-derivatives, **2-TiMe$_2$** is the most active catalyst when combined with [Ph$_3$C][B(C$_6$F$_5$)$_4$]. A good activity is showed by **3-TiMe$_2$** and **5-TiMe$_2$**, closely followed by **7-TiMe$_2$**. **8-TiMe$_2$** is less active, at difference with what observed in liquid monomer with MAO. With these sterically open systems, no simple correlation between ligand structure and activity could be derived.

In the presence of the borate salt [PhNHMe$_2$]-[B(C$_6$F$_5$)$_4$] all the three complexes tested showed almost

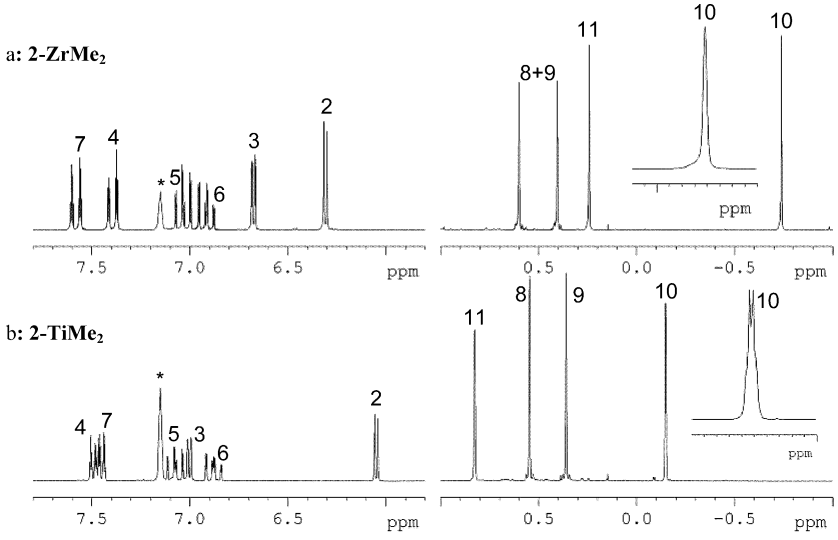

Fig. 1. Aromatic and methyl regions in ^{1}H-NMR spectra of [Me$_2$Si(Ind)(*t*-BuN)]ZrMe$_2$ (**2-ZrMe$_2$**, a) and [Me$_2$Si(Ind)(*t*-BuN)]TiMe$_2$ (**2-TiMe$_2$**, b). Peak assignments according to Chart 2. *, C$_6$D$_5$H, 7.15 ppm.

Table 3
Propylene polymerization: MAO activated catalysts

Run	Catalyst		Cocatalyst	Al/Zr (mol mol^{-1})	Temperature (°C)	Time (min)	Yield (g)	Activity (kg_{pp} ($mmol_{Ti} \times h$)$^{-1}$)	% Triads			Rde (%) [a]	E [b]	B [c]	2,1 (%)	$\overline{M}_w$
	Type	μmol							mm	mr	rr					
1	**1-TiCl$_2$**	2.7	MAO	3000	50	60	35.0	12.9	9.6	38.1	52.3	42.6	0.5	1.4	1.3	1 190 800
2	**1-TiCl$_2$**	5.4	MAO	1000	50	60	26.6	4.9								848 200
3	**1-TiCl$_2$**	5.4	MAO	1000	60	60	59.0	10.9	10.5	39.3	50.2	39.7	0.5	1.4	1.3	650 300
4	**1-TiCl$_2$**	5.4	MAO	1000	70	60	63.1	11.6	10.7	41.3	48.0	37.3	0.5	1.2	1.6	420 100
5	**1-TiCl$_2$**	5.4	MAO	500	70	60	51.4	9.5								446 900
6	**1-TiMe$_2$**	3.0	MAO	1000	60	60	26.8	8.8	10.5	38.9	50.6	40.0	0.5	1.4	1.6	697 900
7	**1-TiMe$_2$**	6.1	MAO	500	60	60	58.6	9.6								710 500
8	**1-TiMe$_2$**	6.1	MAO	500	70	60	27.9	4.6								424 600
9	**2-TiMe$_2$**	6.2	MAO	1000	60	60	24.9	4.1	24.8	38.9	36.3	11.5	1.3	2.4	1.5	135 400
10	**2-TiMe$_2$**	6.2	MAO	500	70	60	14.0	2.3	26.5	37.7	35.8	9.3	1.4	2.7		103 700
11	**3-TiMe$_2$**	3.0	MAO	1000	60	60	18.3	6.2	15.6	33.1	51.3	35.7	0.9	2.9	0.6	550 800
12	**7-TiMe$_2$**	4.9	MAO	1000	60	60	58.0	11.9	29.4	35.5	35.1	5.7	1.7	3.3	1.1	625 700
13	**8-TiMe$_2$**	5.2	MAO	1000	60	30	80.0	30.8	13.8	38.9	47.3	33.6	0.7	1.7	0.7	194 000

Polymerization conditions: **1-L** autoclave, propylene = 300 g, 1 mmol Al(iBu)$_3$.

[a] Rde: racemic dyad excess; % rde = $100([r]-[m]) = \% rr - \% mm$. Positive numbers indicate syndiospecificity, negative ones isospecificity [32,33].

[b] E, enantiomorphic site triad test. $E = 2[mm]/[mr]$ for a syndiotactic polymer; $E = 2[rr]/[mr]$ for an isotactic polymer. $E = 1$ for perfect site control [32,33].

[c] B, Bernoullian triad test. $B = 4[mm][mr]/[mr]^2$. $B = 1$ for perfect Bernoullian distribution with chain-end control [32,33].

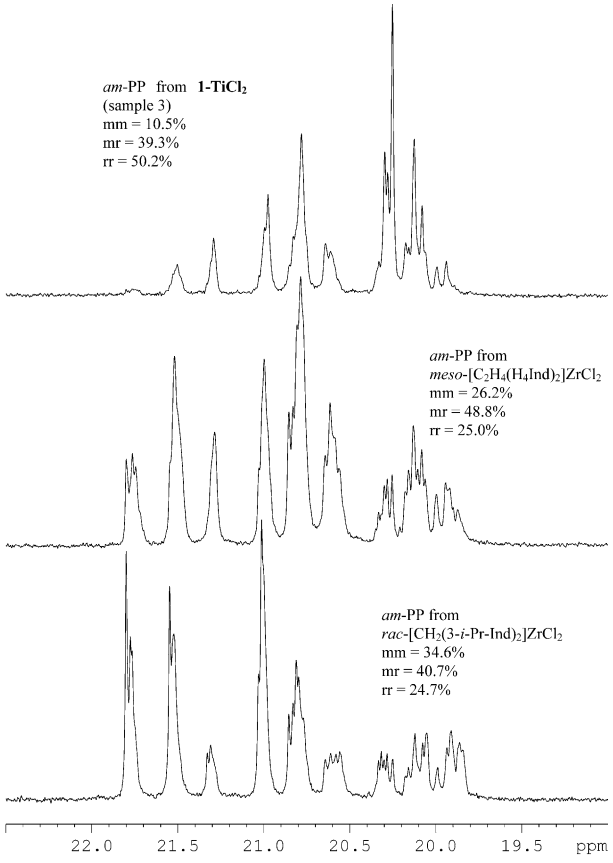

Fig. 2. Methyl pentad region of ^{13}C-NMR spectra ($C_2D_2Cl_4$, 120 °C) of *am*-PP with various degrees of microstructure prepared from **1-TiCl$_2$**–MAO, *meso*-[$C_2H_4(H_4Ind)_2$]$ZrCl_2$–MAO and *rac*-[CH_2(3-*i*-Pr-Ind)$_2$]$ZrCl_2$–MAO in liquid monomer at 60 °C.

the same activity, a little higher than those obtained with MAO, but much lower than in the case of $[Ph_3C][B(C_6F_5)_4]$.

By comparing Table 3 with Table 4, it appears that there is no strong influence on tacticity of propylene concentration (compare runs 11 in Table 3 with 23 in Table 4 for **3-TiMe$_2$**), nor of cocatalyst type: **2-TiMe$_2$**, **3-TiMe$_2$** and **5-TiMe$_2$** show the same or very similar degree of stereocontrol when activated by MAO, $[Ph_3C][B(C_6F_5)_4]$, or $[PhNHMe_2][B(C_6F_5)_4]$.

Even if all the polymers produced are essentially atactic, a microstructure unbalanced towards isotacticity is observed for some of them (isotactoid, amorphous polypropylene, *iam*-PP), while some others are syndiotactic-enriched (syndiotactoid, amorphous polypropylene, *sam*-PP). In particular, precatalysts without any substituent on the Cp ring as **2-TiMe$_2$** [15] and **5-TiMe$_2$** give rise to *iam*-PP ($\%mm > \%rr$), and it also seems that a substituent in position 4 (**5-TiMe$_2$**) could enhance the tendency to isotacticity, as already observed in propylene polymerization in liquid monomer. In the presence of a substituent on the Cp ring (**3-TiMe$_2$**, **6-TiMe$_2$** and **8-TiMe$_2$**) a *sam*-PP is produced ($\%mm < \%rr$). The tendency to isotacticity due to the substituent in position 4 and that to syndiotacticity due to the substituent in position 2 are perfectly balanced in **7-TiMe$_2$**, which has substituents in both positions 2 and 4: the *am*-PP is then almost completely atactic ($\%mm = 28.9 \approx \%rr = 31.0$). The methyl region of the spectra of three *am*-PPs with different microstructures is shown in Fig. 3.

Quite high levels of 2,1-insertions are observed in most samples, while they are practically absent in those from **3-TiMe$_2$** and **8-TiMe$_2$**: these two complexes gave the lowest, albeit not nil, amounts of regiomistakes also in liquid monomer. Interestingly, the borate activators induce a higher concentration of regioerrors compared with MAO.

The molecular weight strongly depends on the substitution of the Cp ring: the complex without any substituent gives polymers of lower molecular weight, while the presence of a methyl group in position 2 determines, as in the case of liquid monomer polymerization, a nearly 3-fold increase in molecular weight. The cocatalyst seems to have some influence on molecular weight, with MAO-activated systems producing *am*-PP of lower molecular weights. This effect is most evident in the case of **3-TiMe$_2$**. If we assume chain transfer to $AlMe_3$ (from MAO) to be the origin of the lower polymer molecular weight, formation of a less reactive Ti–$AlMe_3$ complex could also explain the lower activity of MAO-cocatalyzed versus borate-cocatalyzed systems.

2.3.3. Propylene polymerization in solution: influence of monomer concentration

The influence of propylene concentration in the liquid phase was investigated in toluene at 50 °C on **2-TiMe$_2$**, **3-TiMe$_2$** and **5-TiMe$_2$**, activated by $[Ph_3C][B(C_6F_5)_4]$, in the propylene pressure range of 2–6 bar, corresponding to propylene concentration of 0.9–3.7 mol l^{-1}. The different concentrations were obtained by varying the propylene pressure at constant temperature. The results are collected in Table 5. The catalytic activity clearly increases with propylene concentration in the liquid phase, but the trends are not always linear. **2-TiMe$_2$** shows a nicely linear dependence of activity on [propylene], while **3-TiMe$_2$** displays a clear higher order dependence. Models have been developed to explain such a non-linear dependence [33], although in the present case the available experimental evidence does not allow us to elect one model over the others. In addition, since catalytic activity is influenced by many variables including possibly different catalyst decay rates, a deviation from a linear dependence on monomer concentration is quite easy.

The microstructure, in terms of triad distribution and amount of 2,1 inserted units, and the molecular weight do not seem to change noticeably with monomer concentration.

Table 4
Propylene polymerization in solution with different activators [a]

Run	Catalyst		Cocatalyst	Time (min)	Yield (g)	Activity (kg_{pp} ($mmol_{Ti} \times h$)$^{-1}$)	% Triads			Rde (%) [b]	E [b]	B [b]	2,1 (%)	$\overline{M}_w$
	Type	μmol					mm	mr	rr					
14	1-$TiCl_2$ [c]	1	$[Ph_3C][B(C_6F_5)_4]$	8	5.2	39.1	13.1	52.2	34.7	21.6	0.5	0.7	2.0	
15	**2-$TiMe_2$**	2	$[Ph_3C][B(C_6F_5)_4]$	5	3.2	19.1	38.8	39.7	21.5	−17.3	1.1	2.1	2.4	109 900
16	**3-$TiMe_2$**	1	$[Ph_3C][B(C_6F_5)_4]$	10	1.9	11.3	20.5	45.3	34.2	13.7	0.9	1.4	0.7	398 200
17	**4-$TiMe_2$**	4	$[Ph_3C][B(C_6F_5)_4]$	25	0.4	0.2								
18	**5-$TiMe_2$**	1	$[Ph_3C][B(C_6F_5)_4]$	10	2.2	13.0	42.6	37.6	19.8	−22.8	1.1	2.4	4.8	111 400
19	**6-$TiMe_2$**	2	$[Ph_3C][B(C_6F_5)_4]$	15	0.8	1.6	9.9	46.8	43.3	33.4	0.4	0.8	6.4	58 000
20	**7-$TiMe_2$**	1	$[Ph_3C][B(C_6F_5)_4]$	10	1.6	9.4	28.9	40.1	31.0	2.1	1.4	2.2	2.2	317 800
21	**8-$TiMe_2$**	1	$[Ph_3C][B(C_6F_5)_4]$	10	1.0	6.1	15.5	46.2	38.3	22.9	0.7	1.1	0.5	326 000
22	**3-$TiMe_2$**	3	MAO	60	1.0	0.3	16.7	39.9	43.4	26.7	0.8	1.8	traces	293 400
23	**5-$TiMe_2$**	3	MAO	45	1.7	0.8	40.4	39.0	20.6	−19.8	1.1	2.2	2.5	73 000
24	**6-$TiMe_2$**	8	MAO	60	1.7	0.1	11.0	48.1	40.9	29.9	0.5	0.8	3.9	35 800
25	**2-$TiMe_2$**	5	$[PhNHMe_2][B(C_6F_5)_4]$	10	2.2	2.6	36.3	38.8	24.9	−11.4	1.3	2.4	1.7	82 900
26	**3-$TiMe_2$**	5	$[PhNHMe_2][B(C_6F_5)_4]$	14	2.8	2.4	20.2	44.3	35.5	15.3	0.9	1.5	1.2	508 600
27	**5-$TiMe_2$**	3.75	$[PhNHMe_2][B(C_6F_5)_4]$	15	2.9	3.1	41.1	37.8	21.1	−20.1	1.1	2.4	3.8	105 200

[a] Polymerization conditions: 260 ml Büchi glass autoclave, 100 ml toluene, 0.5 mmol Al(iBu)$_3$ as scavenger in toluene, B/Ti = 1 (mol mol^{-1}), Al/Ti = 1000 (mol mol^{-1}), pressure = 3 bar-g, temperature = 50 °C, precontact in toluene (5 ml): 30 s (time necessary to transfer the catalytic solution into the reactor).

[b] See footnotes of Table 3.

[c] In order to use this dichloride derivative in combination with a borate, **1-$TiCl_2$** was previously alkylated with Al(iBu)$_3$ (Al/Ti = 50 (mol mol^{-1}), aging = 10 min).

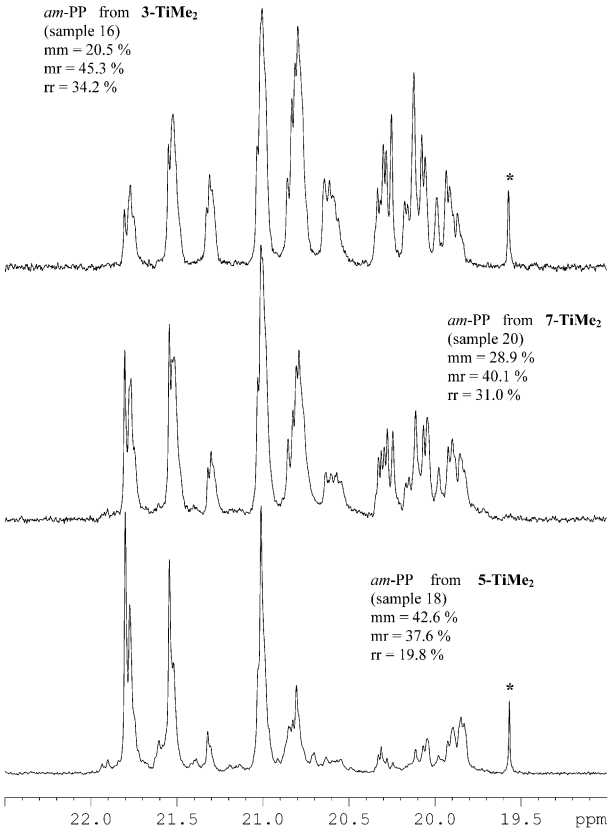

Fig. 3. Methyl pentad region of the ^{13}C-NMR spectra ($C_2D_2Cl_4$, 120 °C) of *am*-PP with various degrees of microstructure prepared from 'constrained geometry' catalytic precursors in solution at 50 °C. *, Toluene.

The molecular weight of a polyolefin (here defined by the average degree of polymerization, $\bar{P}_n$, estimated from $\bar{M}_w$, see Section 3) made with single center catalysts (which operate by coordination polyinsertion mechanism) is given by the ratio between the overall rate of propagation (R_p) and the sum of all rates of chain release reactions (R_r) [32,33,38].

$$\bar{P}_n = \frac{\sum R_p}{\sum R_r}$$

Assuming for simplicity a first order reaction rate with respect to monomer concentration, that is: $R_p = k_p$ [M], when the average degree of polymerization is independent from monomer concentration, as in the present case, then the rate of chain release is first order in monomer: $R_r = k_r$ [M]. Whether this is due to direct β-H transfer to the coordinated monomer or to associative displacement following a unimolecular β-H transfer [38] cannot be established with the data at hand.

2.3.4. Propylene polymerization in solution: effect of polymerization temperature

Tests at different polymerization temperatures were carried out with the same three catalytic systems already used for the study of the effect of monomer concentration. The tests were performed under the same monomer concentration (1.85 mol l^{-1}), by modulation of the propylene pressure determined by Aspen Plus calculation.

The results are collected in Table 6. The catalytic activity seems to increase with the polymerization temperature, but some trends are not completely linear for the reasons described above. For **5-TiMe$_2$** a linear dependence of the catalytic activity from the temperature is observed in the range 20–80 °C, and the Arrhenius plot $\ln(\text{Activity}) = \ln A - \Delta E^{\ddagger}/RT$ gives an overall activation energy $\Delta E^{\ddagger}$ **5-TiMe$_2$** for the polymerization process of 7.35 kcal mol^{-1}. This value is very similar, even if slightly lower, to those obtained with metallocene catalysts (in the range of 10–15 kcal mol^{-1} [39]).

The isotacticity degree shows a slight decrease and the regioinversion content shows a slight increase as the polymerization temperature increases, while the $\bar{M}_w$ strongly decreases. The Arrhenius plots of ln $\bar{P}_n$ (estimated from $\bar{M}_w$, see Section 3) versus $1/T_p$ for the three catalysts are reported in Fig. 4. From the slope of the line the $\Delta\Delta E^{\ddagger}$ (activation energy barrier for chain release) can be calculated for the three catalysts:

$\Delta\Delta E^{\ddagger}$ **2-TiMe$_2$** = 3.4 kcal mol^{-1},

$\Delta\Delta E^{\ddagger}$ **5-TiMe$_2$** = 3.8 kcal mol^{-1},

$\Delta\Delta E^{\ddagger}$ **3-TiMe$_2$** = 6.3 kcal mol^{-1}.

2.3.5. Mechanism of enantioface selectivity

The exact determination of pentad distribution of these samples is difficult, due to the presence of considerable amount of erythro (E) and threo (T) 2,1 units. In isotactic polypropylene, the chemical shift of the methyl of a propylene unit close to the $2,1_E$ unit overlaps with the *mmrr* signal. On the other hand, no assignments are available for the same methyl in a non isotactic environment and for the methyl of a propylene near to a $2,1_T$ unit. It is not yet possible to introduce corrections in the experimental integrals to take into account the presence of signals due to propylene units near to regioerrors.

The experimental pentad distribution for the three samples is reported in Table 7. As these samples have a slight tendency towards isotacticity, to understand what mechanism of enantioface selectivity is operating, the B (for chain end control) and E (for enantiomorphic site control) triad tests were applied, using triads calculated from the experimental pentads. As the E test is close to 1 for all three samples (see Tables 3–6), we can conclude that chiral induction comes mainly form a weak enantiomorphic site control.

Table 5
Propylene polymerization in solution at different monomer concentrations [a]

Run	Catalyst		Pressure (bar-g)	[Propylene]$_{l.p.}$ (mol l^{-1}) [b]	Time (min)	Yield (g)	Activity (kg_{pp} ($mmol_{Ti} \times h$)$^{-1}$)	% Triads			Rde [c]	E [c]	B [c]	2,1 (%)	$\overline{M}_w$
	Type	μmol						mm	mr	rr	%				
28	**2-TiMe$_2$**	1.7	1	0.87	7	0.6	3.0	38.8	39.6	21.7	−17.1	1.1	2.1	2.7	105 200
29	**2-TiMe$_2$**	1.7	2	1.57	7	2.6	13.2								108 300
15	**2-TiMe$_2$**	2	3	2.26	5	3.2	19.1	38.8	39.7	21.5	−17.3	1.1	2.1	2.4	109 900
30	**2-TiMe$_2$**	1.5	4	2.95	5	3.0	24.0								127 300
31	**2-TiMe$_2$**	1	5	3.65	7	3.4	29.1	35.7	39.3	25.0	−10.8	1.3	2.3	1.6	122 500
32	**3-TiMe$_2$**	1.3	1	0.87	15	1.1	3.4	20.7	45.1	34.2	13.5	0.9	1.4	0.5	279 400
33	**3-TiMe$_2$**	1	2	1.57	10	0.8	5.0								420 100
16	**3-TiMe$_2$**	1	3	2.26	10	1.9	11.3	20.5	45.3	34.2	13.7	0.9	1.4	0.5	398 200
34	**3-TiMe$_2$**	1	4	2.95	9	2.7	18.2								365 900
35	**3-TiMe$_2$**	1	5	3.65	5	3.0	36.5	20.0	44.8	35.2	15.2	0.9	1.4	0.5	342 600
36	**5-TiMe$_2$**	1.25	1	0.87	10	1.8	8.5	40.5	38.0	21.5	−18.9	1.1	2.4	3.9	105 200
37	**5-TiMe$_2$**	1	2	1.57	10	0.7	4.2								114 500
18	**5-TiMe$_2$**	1	3	2.26	10	2.2	13.0	42.6	37.6	19.8	−22.8	1.1	2.4	4.8	111 400
38	**5-TiMe$_2$**	1	4	2.95	10	3.2	19.4								106 800
39	**5-TiMe$_2$**	1	5	3.65	10	1.7	10.4	40.7	38.0	21.3	−19.3	1.1	2.4	3.6	109 900

[a] Polymerization conditions: 260 ml Büchi glass autoclave, 100 ml toluene, 0.5 mmol Al(iBu)$_3$ as scavenger in toluene, [Ph_3C][$B(C_6F_5)_4$] as cocatalyst, B/Ti = 1 (mol mol^{-1}), temperature = 50 °C, precontact in toluene (5 ml): 30 s (time necessary to transfer the catalytic solution into the reactor).

[b] Propylene concentration in liquid phase in mol l^{-1}, obtained by interpolation of values calculated from Redlich–Kwong–Soave equations (see Section 3).

[c] See footnotes in Table 3.

Table 6
Propylene polymerization in solution at different temperatures [a]

Run	Catalyst		Pressure (bar-g)	Temperature (°C)	Time (min)	Yield (g)	Activity (kg_{pp} ($mmol_{Ti} \times h$)$^{-1}$)	% Triads			Rde (%) [b]	E [b]	B [b]	2,1 (%)	$\overline{M}_w$
	Type	μmol						mm	mr	rr					
40	**2-TiMe$_2$**	1.7	0.85	21	8	0.7	3.1	37.8	38.5	23.7	−14	1.2	2.4	2.4	190 400
41	**2-TiMe$_2$**	2.0	1.9	46.5	10	2.7	8.0								138 700
42	**2-TiMe$_2$**	1.8	3.3	63	7	2.3	11.1								93 100
43	**2-TiMe$_2$**	1.8	5.0	80	5	1.2	8.2	32.8	42.1	25.1	−7.7	1.2	1.9	2.7	74 400
44	**3-TiMe$_2$**	1.5	0.85	20	10	1.5	6.2	19.9	44.6	35.5	15.6	0.9	1.4	traces	1 036 700
45	**3-TiMe$_2$**	1.5	1.9	44	8	2.0	10.0								433 500
46	**3-TiMe$_2$**	1.5	3.3	65	10	3.8	15.4								253 900
47	**3-TiMe$_2$**	1.5	5.0	80	15	3.6	9.7	19.1	48.6	34.1	15.0	0.8	1.2	1.2	160 600
48	**5-TiMe$_2$**	1.0	0.85	23	12	0.2	1.0	41.8	37.6	20.6	−21.1	1.1	2.4	3.3	210 400
49	**5-TiMe$_2$**	1.0	1.9	42.5	12	0.5	2.8								132 100
50	**5-TiMe$_2$**	2.0	3.3	62	10	1.6	4.8								90 200
51	**5-TiMe$_2$**	1.25	5.0	79	12	1.8	7.0	37.0	40.1	22.9	−14.2	1.1	2.1	4.1	75 800

[a] Polymerization conditions: 260 ml Büchi glass autoclave, 100 ml toluene, 0.5 mmol Al(iBu)$_3$ as scavenger in toluene, [Ph_3C][$B(C_6F_5)_4$] as cocatalyst, B/Ti = 1 (mol mol^{-1}), precontact in toluene (5 ml): 30 s (time necessary to transfer the catalytic solution into the reactor). Propylene concentration in liquid phase: 1.85 mol l^{-1}.
[b] See footnotes of Table 3.

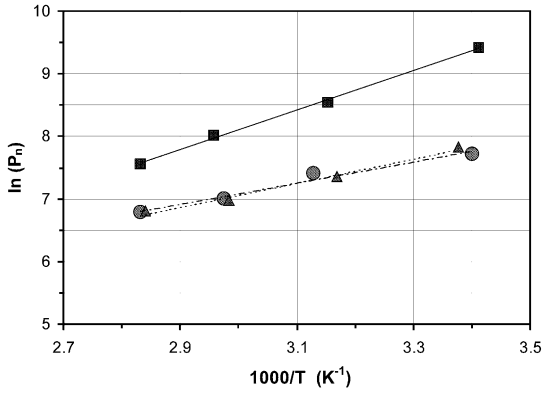

Fig. 4. Arrhenius plots of $\ln(\bar{P}_n)$ vs. $1/T_p$ for **2-TiMe$_2$** (●, $\Delta\Delta E^{\ddagger}_{release} = 3.4$ kcal/mol), **3-TiMe$_2$** (■, $\Delta\Delta E^{\ddagger}_{release} = 6.3$ kcal/mol), and **5-TiMe$_2$** (▲, $\Delta\Delta E^{\ddagger}_{release} = 3.8$ kcal/mol).

This result is confirmed by the application of both the Bernoullian (for enantiomorphic site control) and the (symmetric) Markovian (for chain end control) models to the experimental pentad distribution. The calculated pentads are reported in Table 7 together with the probability parameters b (the probability for the insertion of the preferred enantioface in the Bernoullian model) and $P(r)$ (the probability for the formation of an r diad in the Markovian model). In the Table 7 the values of the least-squares fitting L.S. is also reported.

The L.S. of the Bernoullian fitting is always lower that the L.S. of the Markovian one, confirming the results obtained from the E-test.

In spite of the non perfect fitting between experimental and calculated pentads (likely due to the presence of 2,1 units), this fitting is good enough for the selection of the model [40].

3. Experimental

3.1. General procedures

All operations were performed under nitrogen by using conventional Schlenk-line techniques. Solvents were purified by degassing with N_2 and passing over activated (8 h, N_2 purge, 300 °C) Al_2O_3, and stored under nitrogen. MeLi (Fluka or Aldrich), n-BuLi (Aldrich), HexylLi (Aldrich), Me_2SiCl_2 (Aldrich), $TiCl_4$ (Aldrich), t-BuNH$_2$ (Aldrich), 2-methylindene (Boulder Scientific), t-butylindene (Boulder Scientific), 4,7-dimethylindene (Boulder Scientific), $(Me_4C_5H)SiMe_2(t\text{-BuNH})$ (Boulder Scientific), indene (Aldrich), $B(C_6F_5)_3$ (Boulder Scientific), $[Ph_3C][B(C_6F_5)_4]$ and $[PhNHMe_2][B(C_6F_5)_4]$ (Austin) were used as received. Al(i-Bu)$_3$ (Witco) was used as 1 M toluene solution and MAO (methylalumoxane, Witco) was purchased as a 10 wt% solution in toluene and then used as received (liquid propylene tests) or dried under vacuum to remove most of the free trimethylaluminum and used as 1 M toluene solution. Polymerization grade propylene was obtained from the Basell Ferrara plant. All complexes were isolated by filtration and drying from a toluene solution, and characterized by ^{1}H- and ^{13}C-NMR spectroscopy. Elemental analysis in several cases did not give satisfactory results, due to the limited air stability of these dimethyl complexes.

3.2. ^{1}H- and ^{13}C-NMR analysis

The proton and carbon spectra of ligands and metallocenes were obtained using a Bruker DPX 200 spectrometer operating in the Fourier transform mode at room temperature (r.t.) at 200.13 MHz (^{1}H) and 50.323 MHz (^{13}C). The samples were dissolved in $CDCl_3$ or C_6D_6. The residual peak of $CHCl_3$ or C_6D_5H in the ^{1}H spectra (7.25 and 7.15 ppm, respectively) and the central peak of the solvent in the ^{13}C-NMR spectra (77.00 ppm for $CDCl_3$ and 128.00 ppm for C_6D_6) were used as references. Proton NMR spectra were acquired with a 15° pulse and 2 s of delay between pulses; 16 or 32 transients were stored for each spectrum. The carbon spectra were acquired with a 45° pulse and 6 s of delay between pulses; about 512 transients were stored for each spectrum. $CDCl_3$ (Aldrich, 99.8 atom% D) and C_6D_6 (Aldrich, 99.6 atom% D) were dried over P_4O_{10} or CaH_2, distilled, and stored over activated molecular sieves (4–5 Å).

Carbon and proton NMR spectra of polymers were recorded on a Bruker DPX-400 spectrometer operating at 100.61 MHz in the Fourier transform mode, at 120 °C. The samples were prepared by dissolving 40 mg of polymer (for ^{13}C) or 10 mg (for ^{1}H) in 0.5 ml of 1,1,2,2-tetrachloroethane-d_2 at 120 °C. The peaks of the mmmm pentad (21.8 ppm) and of C_2HDCl_2 (5.95 ppm) were used as internal reference in ^{13}C- and ^{1}H-NMR spectra, respectively. Each carbon NMR spectrum was acquired with a 90° pulse, 12 s of delay between pulses and CPD (waltz 16) to remove ^{1}H–^{13}C coupling. About 3000 transients were stored in 32K data points using a spectral window of 60 ppm. Each proton spectrum was acquired with a 45° pulse, 5 s of delay between pulses. About 1K of transients were stored in 32K data points using a spectral window of 16 ppm.

3.3. Molecular weight measurements

The intrinsic viscosity (I.V.) was measured in tetrahydronaphthalene (THN) at 135 °C. The weight average molecular weights of *am*-PP were obtained from their intrinsic viscosity values and the Mark–Houwink–Sakurada parameters derived by Pearson and Fetters: $[\eta] = 1.85 \times 10^{-4} \times (\bar{M}_w)^{0.737}$ [41].

The average degree of polymerization, $\bar{P}_n$, is estimated from $\bar{M}_w$ by assuming $\bar{M}_w/\bar{M}_n = 2$.

Table 7
Analysis of pentad distribution of samples 18, 24 and 28

Sample		*mmmx*	*rmmr*	*mmrr*	*xmrx*	*rmrm*	*rrrr*	*rrrm*	*mrrm*	B [a]	E [b]	b [c]	$P(r)$ [d]	L.S. [e]
18	Exp	0.3910	0.0299	0.2042	0.1197	0.0522	0.0303	0.0528	0.1199	2.415	1.079			
	Bern	0.4104	0.0343	0.1646	0.1371	0.0685	0.0343	0.0685	0.0823			0.7547		$4.21E-03$
	MK	0.3890	0.0500	0.1000	0.2472	0.1000	0.0130	0.0509	0.0500				0.3374	$3.58E-02$
28	Exp	0.3796	0.0318	0.2096	0.1284	0.0400	0.0351	0.0541	0.1213	2.426	1.114			
	Bern	0.4011	0.053	0.1640	0.1412	0.0706	0.0353	0.0706	0.0820			0.7493		$5.47E-03$
	MK	0.3785	0.0510	0.1020	0.2477	0.1020	0.0141	0.0536	0.0510				0.3446	$3.62E-02$
24	Exp	0.3567	0.0470	0.2033	0.1412	0.0459	0.0353	0.0571	0.1136	2.182	1.055			
	Bern	0.3778	0.0379	0.1619	0.1517	0.0759	0.0379	0.0759	0.0810			0.7335		$4.67E-03$
	MK	0.3579	0.0530	0.1059	0.2484	0.1059	0.0166	0.0593	0.0530				0.3590	$2.96E-02$

[a] $B = 4[mm][rr]/[mr]^2$. Chain end control is identified by $B = 1$.
[b] $E = 2[rr]/[mr]$. Site control is identified by $E = 1$.
[c] b, Probability for the insertion of the preferred enantioface in the Bernoullian model.
[d] $P(r)$, Probability for the formation of an r diad in the Markovian model.
[e] L.S. $= \Sigma_{\text{penteds}}(xxxx_{\text{exp}} - xxxx_{\text{calc}})^2$.

3.4. GC–MS analysis

GC–MS analyses were carried out on a HP 5890-serie 2 gas-chromatograph and a HP 5989B mass spectrometer.

3.5. Determination of monomer concentration

The composition of liquid phase of propylene–toluene mixtures was calculated from the Redlich–Kwong–Soave equations [42–44]. This set of thermodynamic equations was selected among those available in Aspen Plus^{TM} (commercialized by Aspen Technology Inc., Release 9) on the basis of a comparison with the experimental results. The propylene concentration was hence calculated.

3.6. Polymerization in liquid monomer

Batch polymerizations were carried out in a 1-L jacketed stainless-steel autoclave, equipped with magnetically driven stirrer, a 35 ml stainless-steel vial, and connected to a thermostat for temperature control. The reactor was purified by washing with a hexane solution of Al(iBu)$_3$, and then dried by purging with propylene at 80 °C for 1 h. The catalyst–cocatalyst mixture was prepared by dissolving the amount of complex in the required amount of MAO–toluene solution, and aged 10 min at r.t. before being injected into the autoclave.

Al(iBu)$_3$ (1 mmol) and the amount of propylene reported in Table 3 were charged, at r.t., in the autoclave. It was then thermostated at 2 °C below the polymerization temperature and the catalyst system, prepared as reported above, was injected in the autoclave by means of nitrogen pressure through the stainless-steel vial. The temperature was rapidly raised to the polymerization temperature, and the polymerization was carried out at constant temperature, for the time reported in Table 3. After venting the unreacted monomer and cooling the reactor to r.t., the polymer was dried under reduced pressure, at 60 °C.

3.7. Polymerization in solution

Propylene polymerizations were carried out in a 260 ml Büchi glass autoclave equipped with magnetic stirrer, thermocouple and feeding line for the monomer, purified with nitrogen and kept in a thermostatic bath. Toluene (95 ml) and Al(iBu)$_3$ (0.5 mmol) were introduced into the autoclave and warmed to the polymerization temperature, then the autoclave was fluxed with propylene. The catalytic system was separately prepared in 5 ml of toluene by mixing the desired amounts of metallocene and cocatalyst. After about 30 s of stirring at r.t., the solution was introduced into the autoclave under monomer flow. The reactor was closed and pressurized; the pressure was kept constant by feeding propylene. The polymerization was stopped by degasing the reactor and by adding 2 ml of methanol. The polymer was precipitated with 200 ml of acidified methanol, filtered, washed with methanol and dried overnight at 60 °C under reduced pressure.

3.8. Synthesis of [$Me_2Si(Me_4C_5)(t$-BuN)]$TiMe_2$ (**1-$TiMe_2$**)

About 21.5 ml of a 1.6 M solution of MeLi in Et_2O (34.4 mmol) were slowly added at 0 °C to a solution of 2.12 g of (Me_4Cp)Me_2Si(t-BuNH) in 45 ml of diethyl ether. During the addition an increasing turbidity develops with final formation of a white suspension. The mixture was allowed to warm up to r.t. and stirred for 1 h. $TiCl_4$ (0.93 ml, 8.45 mmol) were diluted with 10 ml of pentane. This solution was added to the Li salt suspension in diethyl ether at r.t. (slightly exothermic reaction with gas evolution). The resulting black suspension was stirred at r.t. for 1 h, then brought to dryness under reduced pressure. The black solid obtained (4.26 g) was extracted with 90 ml of toluene and the filtrate evaporated to dryness under reduced pressure to give 1.95 g of a dark brown sticky solid (70% yield). ^{1}H-NMR shows the presence of chemically pure [Me_2-Si(Me_4Cp)(t-BuN)]$TiMe_2$.

^{1}H-NMR (C_6D_6, δ, ppm): 0.43 (s, 6H, Si-C$\underline{H}_3$); 0.50 (s, 6H, Ti-C$\underline{H}_3$); 1.56 (s, 9H, $\underline{t}$-Bu); 1.85 (s, 6H, Cp-C$\underline{H}_3$); 1.96 (s, 6H, Cp-C$\underline{H}_3$).

3.9. Synthesis of [$Me_2Si(Me_4Cp)(t$-BuN)]$ZrMe_2$ (**1-$ZrMe_2$**)

About 12.16 ml of a 1.6 M solution of MeLi in Et_2O (19.46 mmol) were added at r.t. to 1.16 g (4.63 mmol) of (Me_4Cp)Me_2Si(t-BuNH) in 25 ml of Et_2O over about 5 min. The mixture was stirred for 2 h. An increasing turbidity develops with final formation of a white suspension, and then a mixture of 1.08 g of $ZrCl_4$ (4.63 mmol) in 25 ml pentane was quickly added. The mixture was stirred overnight and a brown solution is finally obtained. The reaction mixture is brought to dryness under reduced pressure, and the brown solid was extracted with 60 ml of toluene and then the filtrate was evaporated to dryness under reduced pressure to give 1.52 g of a light brown solid (89% yield). ^{1}H-NMR shows the presence of spectroscopically pure [Me_2-Si(Me_4Cp)(t-BuN)]$ZrMe_2$. The same experiment was repeated at −78 °C, giving a yield of 86%.

^{1}H-NMR (C_6D_6, δ, ppm): −0.01 (s, 6H, Zr–C$\underline{H}_3$); 0.46 (s, 6H, Si–C$\underline{H}_3$); 1.40 (s, 9H, $\underline{t}$-Bu); 1.92 (s, 6H, Cp–C$\underline{H}_3$); 1.97 (s, 6H, Cp–C$\underline{H}_3$).

3.10. Synthesis of [Me_2Si(Ind)(t-BuN)]$TiMe_2$ (**2-$TiMe_2$**)

3.10.1. $IndSiMe_2Cl$

About 37.5 ml of a 2.5 M solution of *n*-BuLi in hexane (93.7 mmol, *n*-BuLi:indene = 1.1) were added dropwise to a solution of indene (11 ml, 84.9 mmol) in 60 ml of Et_2O, previously cooled to −78 °C. At the end of the addition, the yellow slurry was allowed to reach r.t. and stirred for 4 h to give an orange solution. The solvents were evaporated under reduced pressure to give a yellow solid, which was taken up in 75 ml of hexane. The milky suspension was stirred for a few minutes, and the lithium salt of indene (white precipitate) was filtered and washed with hexane (3 × 20 ml). The solid was again slurried in hexane (40 ml) and added to a stirred solution of Me_2SiCl_2 (15.6 ml, 136.8 mmol, Me_2SiCl_2/IndLi = 1.5) in 50 ml of hexane, previously cooled to −78 °C. At the end of the addition, the mixture was allowed to reach r.t. and stirred overnight. The suspension was then filtered, and the filtrate brought to dryness in vacuo to yield a light yellow oil of (1-Ind)$SiMe_2Cl$ free from its vinylic isomer (16.5 g, 89% yield). About 5% of bis(1-indenyl)dimethylsilane (*rac*/*meso* = 1:1.2) is also present.

^{1}H-NMR ($CDCl_3$, δ, ppm): 0.21 (s, 3H, Si–CH_3), 0.26 (s, 3H, Si–CH_3), 3.77 (bt, J = 1.87 Hz, 1H, Cp–H), 6.68 (dd, J = 5.39, 1.87 Hz, 1H, Cp–H), 7.03 (ddd, J = 5.39, 1.87, 0.62 Hz, 1H, Cp–H), 7.19–7.36 (m, 2H, Ar–H), 7.48–7.52 (m, 1H, Ar–H), 7.57–7.61 (m, 1H, Ar–H).

3.10.2. (Ind)$SiMe_2$(t-BuNH)

About 5.6 g of (Ind)$SiMe_2Cl$ (26.8 mmol) in 10 ml Et_2O were slowly added with stirring to a solution of 6.6 ml of *t*-$BuNH_2$ (62.9 mmol, *t*-$BuNH_2$:(Ind)$SiMe_2Cl$ = 2.3) in 50 ml Et_2O and cooled to −78 °C. At the end of the addition, the mixture was allowed to reach r.t. and was stirred 24 h to give a white milky suspension. The solvents were evaporated under reduced pressure, and the residue was extracted with 40 ml of pentane and filtered to remove the white ammonium salt from the soluble product. The filtrate was concentrated in vacuo to give a light lemon yellow oil (5.46 g, 83% yield). ^{1}H-NMR analysis shows the formation of (Ind)$SiMe_2$(*t*-BuNH) as a mixture of two isomers (allilic, 75%; vinilic, 25%).

^{1}H-NMR ($CDCl_3$, δ, ppm, for the indenyl fragment assignment see Chart 2), allylic isomer: −0.01 (s, 3H, Si–CH_3), 0.03 (s, 3H, Si–CH_3), 0.72 (bs, 1H, N–H), 1.28 (s, 9H, *t*-Bu), 3.68 (bt, J = 1.87 Hz, 1H, Cp–H**1**), 6.76 (dd, J = 5.39, 1.87 Hz, 1H, Cp–H), 6.98 (ddd, J = 5.39, 1.87, 0.62 Hz, 1H, Cp–H), 7.15–7.40 (m, 2H, Ar–H), 7.5–7.61 (m, 2H, Ar–H); vinylic isomer: 0.44 (s, 6H, Si(CH_3)$_2$), 0.9 (bs, 1H, N–H), 1.22 (s, 9H, *t*-Bu), 3.47 (bm, 2H, Cp–H**1**), 6.87 (t, J = 1.87 Hz, 1H, Cp–H**2**), 3 aromatic protons overlapped with those of the allylic isomer, 7.77 (d, 1H, Ar–H).

3.10.3. [Me_2Si(Ind)(t-BuN)]$TiMe_2$

About 11.3 ml of a 1.6 M solution of methyllitium in diethyl ether (18.04 mmol) were slowly added at −78 °C to a solution of 1.08 g (4.40 mmol) of (Ind)$SiMe_2$(*t*-BuNH) in 23 ml of diethyl ether. During the addition an increasing turbidity develops with final formation of a yellow suspension. This mixture was allowed to warm to r.t. and stirred for 2 h. $TiCl_4$ (0.5 ml, 4.40 mmol) were diluted in 23 ml of pentane. This solution was added very slowly and cautiously to the Li salt suspension in diethyl ether at r.t. The resulting dark suspension was stirred at r.t. overnight. The reaction mixture was then brought to dryness under reduced pressure. The dark solid was extracted with 60 ml of toluene and then the filtrate was evaporated to dryness under reduced pressure to give 0.99 g of a gray–black solid (70% yield). ^{1}H-NMR confirms formation of [Me_2Si(Ind)(*t*-BuN)]$TiMe_2$.

^{1}H-NMR (C_6D_6, δ, ppm, assignments following Chart 2): −0.15 (q, J = 0.48 Hz, 3H, Ti–CH_3, H**10**), 0.36 (s, 3H, Si–CH_3, H**9**), 0.53 (s, 3H, Si–CH_3, H**8**), 0.82 (q, J = 0.48 Hz, 3H, Ti–CH_3, H**11**), 1.44 (s, 9H, *t*-Bu); 6.05 (d, J = 3.21 Hz, 1H, Cp–H**2**); 6.88 (ddd, J = 8.50, 6.64, 1.04 Hz, 1H, Ar–H**6**); 7.01 (dd, J = 3.21, 0.83 Hz, 1H, Cp–H**3**); 7.07 (ddd, J = 8.50, 6.64, 1.04 Hz, 1H, Ar–H**5**); 7.46 (dq, J = 8.50, 1.04 Hz, 1H, Ar–H**7**); 7.48 (dt, J = 8.50, 1.04 Hz, 1H, Ar–H**4**).

^{13}C-NMR (C_6D_6, δ, ppm, assignments following Chart 2): 1.84 (C**9**–Si); 3.96 (C**8**–Si); 34.31 (CH_3–*t*-Bu); 53.85 (C**11**–Ti); 57.18 (C**10**–Ti); 58.52 (C–*t*-Bu); 91.86 (C**1**), 114.12 (C**3**); 125.48 (C**6**); 125.94 (C**4**); 126.07 (C**5**); 126.84 (C**2**); 127.63 (C**7**); 133.22 (C**3a** or C**7a**); 133.44 (C**7a** or C**3a**).

For additional NMR data see Section 5.

3.11. Synthesis of [Me_2Si(Ind)(t-BuN)]$ZrMe_2$ (**2-$ZrMe_2$**)

About 12.8 ml of a 1.6 M solution of methyllitium in diethyl ether (20.54 mmol) were added slowly at −78 °C to a solution of 1.2 g (4.89 mmol) of (Ind)$SiMe_2$(*t*-BuNH) in 25 ml of diethyl ether. During the addition an increasing turbidity develops with final formation of a yellow suspension. This mixture was allowed to warm to r.t. and stirred for 2 h. $ZrCl_4$ (1.14 g, 4.89 mmol) were slurried in 25 ml of pentane. This suspension was added to the Li salt suspension in diethyl ether at r.t. The resulting brown suspension was stirred at r.t. overnight. The reaction mixture was then brought to dryness under reduced pressure. The brown solid was extracted with 60 ml of toluene and then the filtrate was evaporated to dryness under reduced pressure to give 1.62 g of a beige solid (90% yield). ^{1}H-NMR shows the

presence of spectroscopically pure [Me_2Si(Ind)(*t*-BuN)]$ZrMe_2$.

^{1}H-NMR (C_6D_6, δ, ppm, assignments following Chart 2): −0.74 (s, 3H, Zr–CH$_3$, H**10**), 0.24 (s, 3H, Zr–CH$_3$, H**11**), 0.40 (s, 3H, Si–CH$_3$), 0.60 (s, 3H, Si–CH$_3$), 1.31 (s, 9H, *t*-Bu); 6.31 (d, $J = 3.21$ Hz, 1H, Cp–H**2**); 6.68 (dd, $J = 3.21$, 0.83 Hz, 1H, Cp–H**3**), 6.92 (ddd, $J = 8.29$, 6.74, 1.14 Hz, 1H, Ar–H**6**), 7.03 (ddd, $J = 8.29$, 6.74, 1.14 Hz, 1H, Ar–H**5**), 7.39 (dt $J = 8.29$, 1.14 Hz, 1H, Ar–H**4**); 7.58 (dq, $J = 8.29$, 1.14 Hz, 1H, Ar–H**7**).

For additional NMR data see Section 5.

3.12. Synthesis of [Me_2Si(2-MeInd)(*t*-BuN)]$TiMe_2$ (**3-$TiMe_2$**)

3.12.1. (2-MeInd)$SiMe_2Cl$

About 22.1 ml of *n*-BuLi 2.5 M in hexane (55.25 mmol) were added at −20 °C to a solution of 6.54 g of 2-MeInd (50.23 mmol) in 70 ml of Et_2O. The resulting orange solution was stirred at −20 °C for 15 min, then allowed to warm up to r.t., and stirred overnight. The solvents were removed giving a light orange lithium salt, which was suspended in hexane and filtered; the insoluble in hexane was washed twice with hexane and dried. The lithium salt was suspended in 70 ml of hexane, cooled at −20 °C and added at this temperature to a solution of 9.1 ml of Me_2SiCl_2 (75.02 mmol) in 60 ml of hexane. The resulting light orange mixture was stirred at −20 °C for 15 min, allowed to warm up to r.t., and stirred overnight. The color of the final reaction mixture was white–light yellow. After filtration on G4 filter, the soluble in hexane was concentrated at 40 °C under vacuum giving 8.40 g of a yellow–orange oil as product (75% yield). Purity by GC: 89.1% of target product and about 6.4% of bis(2-Me-1-indenyl)dimethylsilane.

^{1}H-NMR ($CDCl_3$, δ, ppm, for the indenyl fragment assignments see Chart 3): 0.22 (s, 3H, Si–CH$_3$); 0.47 (s, 3H, Si–CH$_3$); 2.36 (bs, 3H, CH$_3$); 3.64 (bs, 1H, H1); 6.70 (bs, 1H, H3); 7.18–7.56 (m, 4H, Ar–H).

3.12.2. (2-MeInd)$SiMe_2$(*t*-BuNH)

About 5.02 g of (2-MeInd)$SiMe_2Cl$ (25.53 mmol) in Et_2O were added at 0 °C to a solution of 4.18 g of *t*-$BuNH_2$ (56.16 mmol) to give a yellow slurry. The mixture was stirred at r.t. for 16 h. The solvents were evaporated under reduced pressure, and the residue extracted with 50 ml of toluene to give, after filtration and evaporation of the solvent, 5.52 g of an orange oil (83% yield). ^{1}H-NMR analysis shows the presence of (2-MeInd)$SiMe_2$(*t*-BuNH) as a mixture of two isomers (allylic, 60.2%, vinylic, 39.8%).

^{1}H-NMR (C_6D_6, δ, ppm), allylic isomer: −0.09 (s, 3H, Si–CH$_3$); 0.11 (s, 3H, Si–CH$_3$); 1.02 (s, 9H, *t*-Bu); 2.14 (s, 3H, CH$_3$); 3.21 (s, 1H, C–H); 6.52 (s, 1H, C–H); vinylic isomer: 0.46 (s, 6H, Si–CH$_3$); 1.1 (s, 9H, *t*-Bu); 2.06 (s, 3H, CH$_3$); 3.05 (s, 2H, CH$_2$); both isomers: 0.37 and 0.65 (bs, 1H, N–H); 6.98–7.82 (m, 8H, Ar–H).

3.12.3. [Me_2Si(2-MeInd)(*t*-BuN)]$TiMe_2$

About 25 ml of MeLi 1.6 M in Et_2O (40 mmol) were added at 0 °C to a solution of 2.53 g of (2-MeInd)$SiMe_2$(*t*-BuNH) (9.75 mmol), the reaction mixture was allowed to warm up to r.t. and stirred 1.5 h. $TiCl_4$ (1.07 ml) in pentane (9.75 mmol) were added very slowly to the dilithium salt (exothermic reaction with gas evolution). After stirring for 2 h, the solvents were removed under reduced pressure, and the crude residue was taken up in 50 ml of toluene, stirred 30 min, and filtered to give, after evaporation of the solvent, 2.68 g of dark brown powder. The powder was slurried in pentane, filtered, and the extract brought to dryness under reduced pressure to give 2.31 g of ochra powder (71% yield). Heat stability tests, in the solid state and in solution of C_6D_6, respectively, for 1 and 2 h at 50 °C, indicate that the complex is more stable in the solid state.

^{1}H-NMR (C_6D_6, δ, ppm, assignments following Chart 3): −0.11 (q, $J = 0.48$ Hz, 3H,Ti–CH$_3$, H**10**); 0.46 (bs, 3H, Si–CH$_3$, H**9**); 0.56 (bs, 3H, Si–CH$_3$, H**8**); 0.85 (q, $J = 0.48$ Hz, 3H, Ti–CH$_3$, H**11**); 1.47 (s, 9H, *t*-Bu); 1.99 (s, 3H, C**2**–CH$_3$); 6.76 (bs, 1H, H**3**); 6.89 (ddd, $J = 8.41$, 6.77, 1.08 Hz, 1H, H**6**); 7.07 (ddd, $J = 8.41$, 6.77, 1.08 Hz,1H, H**5**); 7.44 (dt, $J = 8.41$, 1.08 Hz, 1H, H**4**); 7.51 (dq, $J = 8.41$, 1.08 Hz, 1H, H**7**).

^{13}C-NMR (C_6D_6, δ, ppm, assignments following Chart 3): 5.30 (C**9**–Si); 5.55 (C**8**–Si); 17.98 (C**2**–CH$_3$); 33.85 (CH$_3$–*t*-Bu); 50.82 (C**11**–Ti); 56.57 (C**10**–Ti); 57.55 (C–*t*-Bu); 89.61 (C**1**), 115.64 (C**3**); 124.72 (C**6**); 124.90 (C**4**); 125.17 (C**5**); 127.81 (C**7**); 131.57 (C**3a**); 133.82 (C**7a**); 140.97 (C**2**).

For further NMR data see Section 5.

3.13. Synthesis of [Me_2Si(3-*t*-BuInd)(*t*-BuN)]$TiMe_2$ (**4-$TiMe_2$**)

3.13.1. (3-*t*-BuInd)$SiMe_2Cl$

About 24 ml di *n*-BuLi 2.5 M in hexane (60 mmol) were added at 0 °C to a solution of 9.3 g (10 ml) of *t*-Bu indene (54 mmol) in Et_2O, obtaining a light yellow suspension, and the mixture of reaction was stirred for 2 h at r.t. A 7.16 ml (7.66 g, 59.4 mmol) of Me_2SiCl_2 were dropwise at 0 °C to lithium salt and the suspension was stirred for 2 h at r.t. The solvent was dried in vacuo and the residue was extracted with 50 ml of toluene, obtaining 13.85 g of an orange oil (81% yield). ^{1}H-NMR spectrum confirms formation of (*t*-BuInd)$SiMe_2Cl$, purity 83.8% wt and about 4.0% wt of bis(1-indenyl)dimethylsilane was also present.

^{1}H-NMR (C_6D_6, δ, ppm): −0.05 (s, 3H, Si–CH$_3$); 0.02 (s, 3H, Si–CH$_3$); 1.34 (s, 9H, *t*-Bu); 3.43 (d, J = 2.07 Hz, 1H, C–H); 6.24 (d, J = 2.07, 1H, C–H); 7.07–7.63 (m, 4H, Ar–H). *m/z* (%): 264 (35) [M^+]; 208 (30); 93 (91); 57 (100).

3.13.2. (3-*t*-BuInd)SiMe$_2$(*t*-BuNH)

About 13.85 g of (*t*-BuInd)SiMe$_2$Cl (52.3 mmol) were added at 0 °C to a solution of 8.98 g (12.9 ml) of *t*-BuNH$_2$ in Et$_2$O, obtaining a yellow suspension. At the end of addition the mixture of reaction was warm up to r.t. and stirred overnight. The solvent was dried in vacuo and the residue was extracted with 40 ml of toluene and the filtrate was concentrated in vacuo to give an orange oil (14.39 g, 91% yield). ^{1}H-NMR spectrum shows the presence only of allilic isomer.

^{1}H-NMR (C_6D_6, δ, ppm, for the indenyl fragment assignment see Chart 2): −0.13 (s, 3H, Si–CH$_3$); −0.08 (s, 3H, Si–CH$_3$); 0.38 (bs, 1H, N–H); 0.39 (bs, 1H, N–H); 1.00 (s, 9H, C**3**–*t*-Bu); 1.38 (s, 9H, N–*t*-Bu); 3.33 (d, J = 2.07, 1H, C–H); 6.31 (d, J = 2.07, 1H, C–H); 7.07–7.68 (m, 4H, Ar–H).

3.13.3. [Me$_2$Si(3-*t*-BuInd)(*t*-BuN)]TiMe$_2$

About 34.91 ml of MeLi (48.88 mmol) were dropwise at 0 °C to a solution of 3.64 g (4 ml) of (*t*-BuInd)SiMe$_2$(*t*-BuNH) (12.07mmol) in 25 ml of Et$_2$O, obtaining an orange solution, and the reaction mixture was stirred at r.t. for 2 h. TiCl$_4$ (1.33 ml, 12.07 mmol) were added at r.t. to lithium salt, obtaining a dark suspension (exothermic reaction with gas evolution). After 2 h the solvent was dried in vacuo and the crude residue was extracted with 50 ml of toluene, obtaining 4.4 g of a black sticky solid which was extracted with 40 ml of pentane, the solvent was removed under reduced pressure obtaining 3.02 g of dark brown oil (66% yield).

^{1}H-NMR (C_6D_6, δ, ppm, assignments following Chart 2): −0.12 (q, J = 0.34 Hz, 3H, Ti–CH$_3$, H**10**); 0.38 (s, 3H, Si–CH$_3$, H**9**); 0.63 (s, 3H, Si–CH$_3$, H**8**); 0.99 (q, J = 0.34 Hz, 3H, Ti–CH$_3$, H**11**); 1.45 (s, 9H,N–*t*-Bu); 1.49 (s, 9H, C**3**–*t*-Bu); 6.15 (s, 1H, H**2**); 6.84 (ddd, J = 7.70, 6.67, 0.97 Hz, 1H, H**6**); 7.11 (ddd, J = 7.76, 6.67, 1.07 Hz, 1H, H**5**); 7.53 (dt, J = 8.61, 1.05 Hz, 1H, H**7**); 7.81 (dt, J = 7.70, 1.05 Hz, 1H, H**4**).

^{13}C-NMR (C_6D_6, δ, ppm, assignments following Chart 2): 1.81 (CH$_3$–Si, C**9**); 4.60 (CH$_3$–Si, C**8**), 30.54 (C**3**–CH$_3$–*t*-Bu); 34.19 (C**3**–C–*t*-Bu); 34.29 (N–CH$_3$–*t*-Bu); 54.46 (C**11** C–Ti); 57.89 (C**10**–C Ti); 58.77 (N–C–*t*-Bu); 90.05 (C**1**); 120.98 (C**2**); 124.54 (C**6**); 125.25 (C**5**); 126.08 (C**4**); 127.80 (C**7**); 132.38 (C**3a**); 135.96 (C**7a**); 141.03 (C**3**).

For additional NMR data see Section 5.

3.14. Synthesis of [Me$_2$Si(4,7-Me$_2$Ind)(*t*-BuN)]TiMe$_2$ (**5-TiMe$_2$**)

3.14.1. (4,7-Me$_2$Ind)SiMe$_2$Cl

About 29.26 ml of *n*-BuLi (73.15 mmol) were dropwise at 0 °C to a solution of 9.59 g (10 ml) di 4,7-dimethyl indene (66.5 mmol) in 25 ml di Et$_2$O, obtaining a light yellow suspension. The reaction mixture was stirred at r.t. for 2 h, then the lithium salt was slowly added at 0 °C to a solution of 9.54 g of Me$_2$SiCl$_2$ (8.97 ml, 73.15 mmol) in 20 ml of Et$_2$O, obtaining a white–light yellow suspension. After a night at r.t., the solvent was dried in vacuo, then the residue was exracted with 60 ml di toluene, the filtrate was brought to dryness under reduced pressure, obtaining 15.25 g of an orange oil.

^{1}H-NMR ($CDCl_3$, δ, ppm): 0.32 (s, 3H, Si–CH$_3$); 0.43 (s, 3H, Si–CH$_3$); 2.61 (s, 3H, CH$_3$–Ar); 2.62 (s, 3H, CH$_3$–Ar); 4.05 (m, 1H, C–H); 6.82–6.92 (m, 1H, C–H); 7.05–7.29 (m, 3H, Cp–H + Ar–H).

3.14.2. (4,7-Me$_2$Ind)SiMe$_2$(*t*-BuNH)

About 15.25 g of (4,7-Me$_2$Ind)SiMe$_2$Cl (64.39 mmol) in 40 ml of Et$_2$O, were added at 0 °C to a solution of 15.22 ml (10.59 g, 141.66 mmol) of *t*-BuNH$_2$ in 30 ml of Et$_2$O, obtaining a yellow suspension. After a night at r.t., the suspension was brought to dryness under reduced pressure and the residue was extracted with 50 ml of toluene. The extract was dried in vacuo obtaining 16.01 g of an orange oil. ^{1}H-NMR confirms formation of (4,7-Me$_2$Ind)SiMe$_2$(*t*-BuNH).

^{1}H-NMR ($CDCl_3$, δ, ppm): −0.043 (bs, 3H, Si–CH$_3$); 0.05 (bs, 3H, Si–CH$_3$); 0.64 (bs, 1H, N–H); 1.22 (s, 9H, *t*-Bu); 2.48 (s, 3H, CH$_3$); 2.51 (s, 3H, CH$_3$); 3.74 (t, J = 1.87, 1H, C–H); 6.74 (dd, J = 5.45, 1.87 Hz, 1H, C–H); 6.91–7.03 (m, 3H, Ar–H + C–H).

3.14.3. [Me$_2$Si(4,7-Me$_2$Ind)(*t*-BuN)]TiMe$_2$

About 44.41 ml of MeLi (62.17 mmol) were dropwise at 0 °C to a solution of 4.2 g of (4,7-Me$_2$Ind)SiMe$_2$(*t*-BuNH) (5 ml, 15.35 mmol) in 40 ml of Et$_2$O, obtaining a yellow–orange solution, the reaction mixture was stirred at r.t. for 1 h. TiCl$_4$ (1.69 ml, 2.91 g, 15.35 mmol) were added at r.t. to lithium salt, obtaining a brown suspension (light exothermic reaction with gas evolution). After 1 h the solvent was dried in vacuo and the residue was extracted with 50 ml of toluene, obtaining 3.43 g of a dark brown oil, which resulted to be the desired product (61% yield). Purity by ^{1}H-NMR: 95.71% wt. Traces of starting ligand (2.75% wt) were also present.

^{1}H-NMR (C_6D_6, δ, ppm, assignments following Chart 2): −0.19 (q, J = 0.54 Hz, 3H, Ti–CH$_3$, H**10**); 0.39 (q, J = 0.34 Hz, 3H, Si–CH$_3$, H**9**); 0.57 (q, J = 0.34 Hz, 3H, Si–CH$_3$, H**8**); 0.78 (q, J = 0.54 Hz, 3H, Ti–CH$_3$, H**11**); 1.47 (s, 9H, *t*-Bu); 2.25 (s, 3H, CH$_3$–C**7**); 2.31 (s, 3H, CH$_3$–C**4**); 6.19 (d, J = 3.40 Hz, 1H, H**2**);

6.71 (dq, $J = 6.89$, 0.93 Hz, 1H, H**6**); 6.83 (dq, $J = 6.89$, 0.93 Hz, 1H, H**5**); 7.09 (d, $J = 3.40$ Hz, 1H, H**3**).

^{13}C-NMR (C_6D_6, δ, ppm, assignments following Chart 2): 3.48 (CH_3–Si, C**9**); 5.71 (CH_3–Si, C**8**);19.1 (CH_3–C**4**); 22.8 (CH_3–C**7**); 34.36 (CH_3–*t*-Bu); 52.03 (CH_3–Ti, C**11**); 56.52 (CH_3–Ti, C**10**); 58.59 (C–*t*-Bu); 92.58 (C**1**); 112.32 (C**3**); 125.71 (C**5**); 126.71 (C**6**), 128.35 (C**2**); 132.49 (C**4**); 132.55 (C**7a**); 134.73 (C**3a**); 135.51 (C**7**).

For further NMR data see Section 5.

3.15. Synthesis of [Me_2Si(3-PhInd)(*t*-BuN)]$TiMe_2$ (**6-$TiMe_2$**)

3.15.1. 1-Phenylindene

About 24.13 ml (72.40 mmol) of PhMgBr were added dropwise to a solution of 6.45 g (48.27 mmol) of 1-indanone in 35 ml of Et_2O, previously cooled at −78 °C, obtaining a grey suspension. The mixture of reaction was allowed to warm up to r.t. in about 4 h and subsequently stirred overnight. The ^{1}H-NMR spectrum showed the formation of the 1-Ph-indanol. Then the solvent was evaporated under reduced pressure, the residue was dissolved in 40 ml of toluene and were added some crystals of *p*-toluenesolfonic acid. After 1.5 h the mixture of reaction was extracted with a solution aqueous of $NaHCO_3$ (2 × 50 ml), then with water (2 × 50 ml). The organic layer was dried over Na_2SO_4. Filtration followed by removal of the solvent, resulted in the isolation of 7.79 g of a yellow–orange oil and the ^{1}H-NMR spectrum confirm the formation of product target (71% yield).

^{1}H-NMR ($CDCl_3$, δ, ppm): 3.56 (d, $J = 2.15$ Hz, 2H, CH_2); 6.64 (t, $J = 2.15$ Hz, 1H, C–H); 7.28–7.60 (m, 9H, Ar–H).

3.15.2. (3-PhInd)$SiMe_2Cl$

About 13.8 ml (34.49 mmol) of *n*-BuLi were added dropwise at 0 °C to a solution of 7.79 g (34.08 mmol) of 1-PhInd in 35 ml of Et_2O, obtaining a red brown solution, which was stirred 4 h at r.t. Then the litium salt was siphoned at 0 °C in a solution of 4.22 ml (4.5 g, 34.49 mmol) of Me_2SiCl_2 in 20 ml of Et_2O. The dark yellow suspension obtained was stirred overnight at r.t., then the solvents were dried in vacuo and the crude (12.27 g) was extracted with 50 ml of toluene, obtaining 9.71 g of an orange oil (82% yield). ^{1}H-NMR analysis confirm the formation of (3-PhInd)$SiMe_2Cl$. Purity by ^{1}H-NMR: 81.89% wt.

^{1}H-NMR ($CDCl_3$, δ, ppm): 0.29 (s, 3H, Si–CH_3); 0.34 (s, 3H, Si–CH_3); 3.90 (d, $J = 2.15$ Hz, 1H, C–H); 6.75 (d, $J = 2.15$ Hz, 1H, C–H); 7.26–7.78 (m, 9H, Ar–H).

3.15.3. (3-PhInd)$SiMe_2$(*t*-BuNH)

About 9.71 g (34.09 mmol) of (3-PhInd)$SiMe_2Cl$ in 35 ml of Et_2O, obtained as reported above, were added at 0 °C to a solution of 7.68 ml of *t*-$BuNH_2$ in 25 ml of Et_2O and the orange suspension obtained was stirred overnight at r.t. The solvent was evaporated under reduced pressure and the crude (14.18 g) was extracted with 50 ml of toluene, the filtrate was dried in vacuo obtaining 10.41 g of a dark orange oil (67% yield). Purity by ^{1}H-NMR: 70.32% wt.

^{1}H-NMR ($CDCl_3$, δ, ppm): 0.07 (s, 3H, Si–CH_3); 0.11 (s, 3H, Si–CH_3); 0.81 (bs, 1H, N–H); 1.32 (s, 9H, *t*-Bu); 3.82 (d, $J = 2.15$ Hz, 1H, C–H); 6.84 (d, $J = 2.15$ Hz, 1H, C–H); 7.25–7.83 (m, 9H, Ar–H).

3.15.4. [Me_2Si(3-PhInd)(*t*-BuN)]$TiMe_2$

About 35.25 ml (56.40 mmol) of MeLi 1.6 M in Et_2O, were added at 0 °C to a solution of 4.51 g (14.03 mmol) of (3-Ph Ind)$SiMe_2$(*t*-BuNH), obtained as reported above, in 25 ml of Et_2O, the solution red–orange obtained was stirred 1h at r.t. To the lithium salt were added 1.54 ml (14.03 mmol) of $TiCl_4$ in 5ml of pentane (exothermic reaction with gas evolution). The dark brown suspension obtained was stirred 1 h at r.t. The solvents were evaporated under reduced pressure, the crude (9.45 g) was extracted with 50 ml of toluene, the dark brown suspension obtained was filtrated and the filtrate dried in vacuo obtaining 4.91 g of product target as a dark brown sticky solid (79% yield). Purity by ^{1}H-NMR: 89.65% wt.

^{1}H-NMR (C_6D_6, δ, ppm, assignments following Chart 2): 0.0065 (bs, 3H, Ti–CH_3, H**10**); 0.42 (s, 3H, Si–CH_3, H**9**); 0.61 (s, 3H, Si–CH_3, H**8**); 0.68 (bs, 3H, Ti–CH_3, H**11**); 1.45 (s, 9H, *t*-Bu); 6.39 (s, 1H, H**2**); 6.92 (ddd, $J = 8.61$, 6.65, 0.98 Hz, 1H, H**6**); 7.08–7.18 (m, 2H, H**5** + H**para**); 7.21–7.31 (m, 1H, H**meta**); 7.53 (dt, $J = 8.61$, 0.98 Hz, 1H, H**7**); 7.63–7.68 (m, 1H, H**ortho**); 7.96 (dt, $J = 8.61$, 0.98 Hz, 1H, H**4**).

^{13}C-NMR (C_6D_6, δ, ppm, assignments following Chart 2): 1.82 (C**9**–Si); 4.09 (C**8**–Si); 34.42 (CH_3–*t*-Bu); 56.33 (C**10**–Ti); 58.97 (C–*t*-Bu); 59.10 (C**11**–Ti); 92.95 (C**1**); 124.54 (C**2**); 124.62 (C**4**); 125.44 (C**6**); 126.65 (C**5**); 128.00 (C**7**); 128.60 (C**para**); 128.64 (C**ortho**); 129.03 (C**meta**); 129.62 (C**3**); 131.46 (C**3a**); 134.56 (C**7a**); 136.37 (C–C**3**).

For additional NMR data see Section 5.

3.16. Synthesis of [Me_2Si(2-Me-4-PhInd)(*t*-BuN)]$TiMe_2$ (**7-$TiMe_2$**)

3.16.1. (2-Me-4-PhInd)$SiMe_2Cl$

About 6.54 ml (16.34 mmol) of *n*BuLi were added dropwise at 0 °C to a yellow solution of 3.21 g (15.56 mmol) of 2-Me-4-PhIndene in 25 ml of Et_2O, obtaining immediately the formation of a yellow ochre suspension. After 30 min of stirring at r.t., 1.96 ml (16.03 mmol) of

Me_2SiCl_2 dissolved in 6 ml of Et_2O were added at 0 °C to the lithium salt. The resulting light yellow suspension was stirred 1 h at r.t. Then the solvents were dried in vacuo and the crude, 5.21 g, was extracted with 40 ml of toluene and the filtrate evaporated to dryness under reduced pressure to give 4.15 g of an orange oil (77% yield). Purity by ^{1}H-NMR: 86.15% wt, 13.85% wt of (2-Me-4-PhInd)$_2$Me$_2$Si.

^{1}H-NMR ($CDCl_3$, δ, ppm): 0.21 (s, 3H, Si–CH$_3$); 0.44 (s, 3H, Si–CH$_3$); 2.28 (bs, 3H, CH$_3$); 3.67 (s, 1H, C–H); 6.82 (s, 1H, C–H); 7.16–7.59 (m, 8H, Ar–H).

3.16.2. (2-Me-4-PhInd)SiMe$_2$(t-BuNH)

About 3.27 ml (30.34 mmol) of t-BuNH_2 dissolved in 10 ml of Et_2O were added at −5 °C to a yellow solution of 4.15 g (13.88 mmol) of (2-Me-4-PhInd)SiMe_2Cl, obtained as described above, in 25 ml of Et_2O. The resulting yellow suspension was allowed to reach r.t. and stirred overnight. Then the solvents were evaporated under reduced pressure and the crude, 6 g, was extracted with 50 ml of toluene. The filtrate was concentrated in vacuo to give 4.41 g of an orange oil. The ^{1}H-NMR analysis shows the formation of (2-Me-4-PhInd)Si-Me$_2$(t-BuNH) (97% yield) as a mixture of two isomers (allylic, 90.29%; vinilic, 9.71%).

^{1}H-NMR ($CDCl_3$, δ, ppm): 0.00 (s, 3H, Si–CH$_3$); 0.18 (s, 3H, Si–CH$_3$); 0.64 (bs, 1H, N–H); 1.22 (s, 9H, t-Bu); 2.29 (d, $J = 1.37$ Hz, 3H, CH$_3$); 3.50 (s, 1H, C–H); 6.75 (m, 1H, C–H) 7.12–7.62 (m, 8H, Ar–H).

3.16.3. [Me$_2$Si(2-Me-4-PhInd)(t-BuN)]TiMe$_2$

About 34.02 ml (54.43 mmol) of MeLi 1.6 M in Et_2O were added at 0 °C to a yellow solution of 4.51 g (13.44 mmol) of (2-Me-4-PhInd)SiMe_2(t-BuNH) in 15 ml of Et_2O, obtaining an orange suspension which was stirred subsequently 30 min at r.t. Then to a lithium salt were added at r.t. $TiCl_4$ (1.49 ml, 2.58 g, 13.44 mmol) dissolved in 10 ml of pentane (exothermic reaction with gas evolution). This black suspension obtained was stirred 1 h. The solvents were dried in vacuo and the crude, 8.44 g, was extracted with 50 ml of toluene. The filtrate was concentrated in vacuo to give 5.58 g of product target as a black sticky solid (86% yield).

^{1}H-NMR (C_6D_6, δ, ppm, assignments following Chart 2): 0.005 (bs, 3H, Ti–CH$_3$, H**10**); 0.47 (s, 3H, Si–CH$_3$, H**9**); 0.60 (s, 3H, Si–CH$_3$, H**8**); 0.85 (bs, 3H, Ti–CH$_3$, H**11**);1.48 (s, 9H, t-Bu); 1.95 (s, 3H, C**2**–CH$_3$); 6.97 (ddd, $J = 8.61$, 6.85 Hz, 1H, H**6**); 7.20 (s, 1H, H**3**), 7.11–7.32 (m, 4H, H**5**, H**para**, H**meta**); 7.52 (dt, $J = 8.61$, 0.98 Hz, 1H, H**7**); 7.62–7.69 (m, 1H, H**ortho**).

^{13}C-NMR (C_6D_6, δ, ppm, assignments following Chart 2): 5.58 (Si–C**9**); 6.00 (Si–C**8**); 18.51 (C**2**–CH$_3$); 34.38 (CH$_3$–t-Bu); 51.88 (Ti–C**11**); 57.62 (Ti–C**10**); 58.08 (C–t-Bu); 89.99 (C**1**); 115.73 (C**3**); 125.35 (C**5**); 125.75 (C**6**); 126.26 (C**7**); 127.82 (C**para**); 128.62 (C**ortho**); 128.98 (C**meta**); 130.69 (C**3a**); 135.14 (C**7a**); 139.17 (C**4**); 141.08 (C–C**4**); 141.90 (C**2**).

For additional NMR data see Section 5.

3.17. Synthesis of [Me$_2$Si(2-Me-Benz[e]Ind)(t-BuN)]TiMe$_2$ (**8-TiMe$_2$**)

3.17.1. (2-Me-Benz[e]Ind)SiMe$_2$Cl

About 8.62 ml (21.56 mmol) of HexylLi were added dropwise at 0 °C to a yellow solution of 3.7 g of 2-Me-benz[e]indene (20.53 mmol) in 12 ml of Et_2O and the resulting light yellow suspension was stirred 30 min at r.t. Then to the lithium salt cooled to 0 °C, were added 2.59 ml (2.76 g, 21.15 mmol) of Me_2SiCl_2 dissolved in 7 ml of Et_2O. The mixture of reaction, a yellow suspension, was stirred 1h at r.t. The solvents were evaporated under reduced pressure, and the crude 6.12 g, was extracted with 50 ml of toluene. The filtrate was evaporated to dryness under reduced pressure to give 4.26 g of (2-Me-3-H-cyclopenta[a]naphthalene)SiMe_2Cl as an orange oil (69% yield). Purity by ^{1}H-NMR: 91.21% wt of target product and 8.79% wt of bis(2-Me-3-H-ciclopenta[a]naphthalen)SiMe_2.

^{1}H-NMR ($CDCl_3$, δ, ppm): 0.16 (s, 3H, Si–CH$_3$); 0.40 (s, 3H, Si–CH$_3$); 2.42 (d, $J = 1.37$ Hz, 3H, CH$_3$); 3.82 (s, 1H, C–H); 7.25–8.17 (m, 7H, Ar–H + Cp–H).

3.17.2. (2-Me-Benz[e]Ind)SiMe$_2$(t-BuNH)

About 3.68 ml (34.34 mmol) of t-BuNH_2 in 10 ml of Et_2O were added dropwise at 0 °C to a yellow solution of 4.26 g (15.61 mmol) of (2-Me-3-H-cyclopenta[a]naphthalene)SiMe_2Cl, as obtained above, in 25 ml of Et_2O, obtaining a light yellow suspension which was stirred overnight at r.t. The solvents were evaporated under reduced pressure, and the crude 6.46 g, was extracted with 40 ml of toluene. The filtrate was evaporated to dryness under reduced pressure to give 4.57 g of an orange oil (95 5 yield). The ^{1}H-NMR spectrum shows the formation of (2-Me-Benz[e]Ind)Si-Me$_2$(t-BuNH) as a mixture of two isomers (allylic, 95.16%; vinilic, 4.84%).

^{1}H-NMR ($CDCl_3$, δ, ppm): −0.08 (s, 3H, Si–CH$_3$); 0.14 (s, 3H, Si–CH$_3$); 0.66 (bs, 1H, N–H); 1.23 (s, 9H, t-Bu); 2.41 (d, $J = 1.37$ Hz, 3H, CH$_3$); 3.66 (s, 1H, C–H); 7.17–8.17 (m, 7H, Ar–H + Cp–H).

3.17.3. [Me$_2$Si(2-Me-Benz[e]Ind)(t-BuN)]TiMe$_2$

About 37.36 ml of MeLi (59.78 mmol) were added at 0 °C to a yellow suspension of 4.57 g (14.76 mmol) of (2-Me-Benz[e]Ind)SiMe_2(t-BuNH) in 15 ml of Et_2O, obtaining a red–orange solution which was stirred 1 h at r.t. Then to the lithium salt was added a solution of 1.63 ml (14.76 mmol) of $TiCl_4$ in 8 ml of pentane, (exhotermic reaction with gas evolution). After 1h the black suspension was dried in vacuo and the crude, 9.22 g was extracted with 40 ml of toluene. The filtrate was

evaporated to dryness under reduced pressure to give 5.14 g of target product as a green powder (87% yield). Purity evaluated by ^{1}H-NMR: $\geq 96\%$ wt.

^{1}H-NMR (C_6D_6, δ, ppm, assignments following Chart 3): −0.33 (bs, 3H, Ti–CH$_3$, H**10**); 0.49 (s, 3H, Si–CH$_3$, H**9**); 0.60 (s, 3H, Si–CH$_3$, H**8**); 0.83 (bs, 3H, Ti–CH$_3$, H**11**); 1.46 (s, 9H, *t*-Bu); 2.06 (s, 3H, C**2**–CH$_3$); 7.21 (d, $J = 8.19$ Hz, 1H, H**6**); 7.30 (s, 1H, H**3**); 7.44 (d, $J = 8.19$ Hz, 1H, H**7**); 7.19–7.46 (m, 2H, H**c**, H**b**); 7.57 (dm, $J = 7.83$ Hz, 1H, H**d**); 8.02 (dm, $J = 8.02$ Hz, 1H, H**a**).

^{13}C-NMR (C_6D_6, δ, ppm, assignments following Chart 3): 5.71 (Si–C**9**); 6.01 (Si–C**8**); 18.42 (C**2**–CH$_3$); 34.37 (CH$_3$–*t*-Bu); 50.80 (Ti–C**11**); 56.71 (Ti–C**10**); 57.41 (C–*t*-Bu); 92.62 (C**1**); 114.86 (C**3**); 123.62 (C**a**); 124.83 (C**7**); 126.42 (C**c**); 126.84 (C**6**); 127.25 (C**b**); 129.05 (C**d**); 129.22 (C**3a** or C**5**); 131.21 (C**4**); 132.35 (C**5** or C**3a**); 132.55 (C**7a**); 139.85 (C**2**).

For further NMR data see Section 5.

4. Conclusions

We have described here a facile, highly efficient, one-pot synthesis of 'constrained geometry' Group 4 metal dimethyl complexes, by the reaction of the ligand with a 2-fold excess of MeLi, and $MtCl_4$ (Mt = Ti, Zr). The ^{1}H-NMR and COSY 2D-NMR spectra of the complexes confirm the presence of through-metal proton–proton coupling for the metal-bound methyl groups, and coupling of Ti-methyl protons with protons on the Cp ring.

The dimethyl titanium indenyl amido complexes bearing different substituents on the indenyl ring were tested in propylene polymerization in combination with different cocatalysts. The aim of the work was to compare catalytic activity and polymers properties, and to verify whether indenyl ring substituents, cocatalysts, monomer concentration and polymerization temperature affect catalyst performance.

Some general conclusions can be drawn. The substituents on the indenyl ring, and in particular their position, affect catalytic activity and molecular weight. The stereoselectivity of the catalyst (the tacticity of the polymer) varies only slightly, while the regioselectivity is modified to a substantial extent by indenyl substitution. Catalytic activity is strongly dependent on the type of cocatalyst, with borates being much more effective as activators compared with MAO. In addition, higher molecular weights are produced by the borates. While the tacticity of *am*-PP does not seem to be affected by the type of cocatalyst, the borates produce a higher content of regioirregularities compared with MAO. The polymer molecular weight is independent from the monomer concentration, but, as usual with homogeneous transition metal catalysts, decreases as the polymerization temperature increases. The rate of chain release is first order in monomer. No influence of monomer concentration or polymerization temperature on microstructure could be found, with the exception of **2-Me$_2$**–MAO. Chiral induction comes mainly from a weak enantiomorphic site control. The influence of ligand structure on regioselectivity and copolymerization performance deserves a deeper investigation. We have pursued other ligand variations on this type of complexes, and will report the results in a following study.

5. Supporting information

Detailed NMR analysis and 2D-NMR spectra of the complexes **2-ZrMe$_2$** and **2-TiMe$_2$-8-TiMe$_2$**.

Acknowledgements

We thank Anna Droghetti for the synthesis of IndSiMe$_2$NH*t*-Bu, Marcello Colonnesi for the ^{1}H-NMR spectra and Fabrizio Piemontesi for helpful discussions on-NMR assignments.

References

[1] L. Resconi, in: W. Kaminsky, J. Scheirs (Eds.), Metallocene Catalysts, vol. 1, Wiley, 1999, p. 467.
[2] L. Resconi, G. Moscardi, R. Silvestri, D. Balboni, PCT International Application WO 00/01738, Montell, Italy 2000.
[3] R. Silvestri, L. Resconi, A. Pelliconi, European Patent Application 697 436 B1, Montell, Italy 1995.
[4] R. Silvestri, P. Sgarzi, Polymer 39 (1998) 5871.
[5] Z.-G. Wang, R.A. Phillips, B.S. Hisiao, J. Polym. Sci. Polym. Phys. 38 (2000) 2580.
[6] R.A. Phillips, R.L. Jones, Macromol. Chem. Phys. 200 (1999) 1912.
[7] J.C. Stevens, F.J. Timmers, D.R. Wilson, G.F. Schmidt, P.N. Nickias, R.K. Rosen, G.W. Knight, S.Y. Lai, European Patent Application 0 416 815 A2, Dow Chemical Company 1990.
[8] R.K. Rosen, B.W. Kolthammer, International Patent Application WO 95/19984, Dow Chemical Company, 1995.
[9] W.A. Herrmann, M.J.A. Morawietz, J. Organomet. Chem. 482 (1994) 169.
[10] D.W. Carpenetti, L. Kloppenburg, J.T. Kupec, J.L. Petersen, Organometallics 15 (1996) 1572.
[11] F. Amor, J. Okuda, J. Organomet. Chem. 520 (1996) 245.
[12] J. Okuda, T. Eberle, in: A. Togni, R.L. Halterman (Eds.), Half-Sandwich Complexes as Metallocene Analogs, vol. 1, Wiley-WCH, Weinheim, 1998, p. 415.
[13] A.L. McKnight, R.M. Waymouth, Chem. Rev. 98 (1998) 2587.
[14] J.A.M. Canich, US Patent 5 504 169, Exxon 1996.
[15] A.L. McKnight, M.A. Masood, R.M. Waymouth, D.A. Straus, Organometallics 16 (1997) 2879.
[16] D.v. Leusen, D.J. Beetstra, B. Hessen, J.H. Teuben, Organometallics 19 (2000) 4084.
[17] P.-J. Sinnema, B. Hessen, J.H. Teuben, Macromol. Rapid Commun. 21 (2000) 565.

[18] Y.-X. Chen, T.J. Marks, Chem. Rev. 100 (2000) 1391.
[19] T. Shiomura, T. Asanuma, N. Inoue, Macromol. Rapid Commun. 17 (1996) 9.
[20] D. Balboni, I. Camurati, G. Prini, L. Resconi, S. Galli, P. Mercandelli, A. Sironi, Inorg. Chem. 40 (2001) 6588.
[21] D. Balboni, G. Prini, M. Rinaldi, L. Resconi, Am. Chem. Soc. Polym. Prep. 41 (2000) 456.
[22] L. Resconi, D. Balboni, G. Prini, WO 99/36427, Montell, Italy 1999.
[23] L. Resconi, PCT International Application WO 00/75151, Montell, Italy 2000.
[24] Y.-X. Chen, T.J. Marks, Organometallics 16 (1997) 3649.
[25] H. Gunther, NMR Spectroscopy, Wiley, Chichester, New York, 1980, p. 189.
[26] A.G. Palmer, J. Cavanagh, P.E. Wright, M. Rance, J. Magn. Reson. 93 (1991) 151.
[27] L.E. Kay, P. Keifer, T. Saarinen, J. Magn. Reson. 114 (1992) 10663.
[28] W. Wilker, D. Leibfritz, R. Kerssebaum, W. Bermel, J. Magn. Reson. 33 (1993) 1835.
[29] R.E. Hurd, Magn. Reson. 87 (1990) 422.
[30] J. Jeener, B.H. Meier, P. Bachmann, R.R. Ernst, J. Chem. Phys. 71 (1979) 4546.
[31] W. Spaleck, M. Antberg, J. Rohrmann, A. Winter, B. Bachmann, P. Kiprof, J. Behm, A. Hermann, Angew. Chem. Int. Ed. Engl. 31 (1992) 1347.
[32] L. Resconi, L. Abis, G. Franciscono, Macromolecules 25 (1992) 6814.
[33] L. Resconi, L. Cavallo, A. Fait, F. Piemontesi, Chem. Rev. 100 (2000) 1253.
[34] Y.-X. Chen, M.V. Metz, L. Li, C.L. Stern, T.J. Marks, J. Am. Chem. Soc. 120 (1998) 6287.
[35] L. Jia, X. Yang, C.L. Stern, T.J. Marks, Organometallics 16 (1997) 842.
[36] Y.-X. Chen, C.L. Stern, S. Yang, T.J. Marks, J. Am. Chem. Soc. 118 (1996) 12451.
[37] J.C.W. Chien, W. Song, M.D. Rausch, J. Polym. Sci. Part A: Polym. Chem. 32 (1994) 2387.
[38] Z. Liu, E. Somsook, C.B. White, K.A. Rosaaen, C.R. Landis, J. Am. Chem. Soc. 123 (2001) 11193.
[39] L. Resconi, F. Piemontesi, I. Camurati, O. Sudmeijer, I.E. Nifantev, P.V. Ivchenko, L.G. Kuzmina, J. Am. Chem. Soc. 120 (1998) 2308.
[40] V. Busico, R. Cipullo, Prog. Polym. Sci. 26 (2001) 443.
[41] D. Pearson, L. Fetters, L. Younghouse, J. Mays, Macromolecules 21 (1988) 478.
[42] G. Soave, Chem. Eng. Sci. 27 (1972) 1196.
[43] A. Peneloux, E. Rauzy, R. Freze, Fluid Phase Equilib. 8 (1982) 7.
[44] J. Schwartzentruber, H. Renon, Ind. Eng. Chem. Res. 28 (1989) 1049.